Numerical Study of Building Geometry (GEO) on Outdoor Ventilation for Singapore's High-rise Residential Estates

Rou-Xuan Lee[*1], Steve Kardinal Jusuf[2], Nyuk-Hien Wong[3]

[1,2,3]Department of Building, School of Design and Environment, National University of Singapore
4 Architecture Drive, Singapore 117566, Singapore

[*1]g0800515@u.nus.edu; [2]steve.kj@nus.edu.sg; [3]bdgwnh@nus.edu.sg

***Abstract*-Geometry (GEO) is one of the urban morphological variables that has effects on microclimate within the urban canopy level (UCL). It is usually quantified in previous researches by different aspect ratios, which have a basis on the buildings' individual height (H), width between each other (W) and their buildings' longitudinal length (L), e.g. H/W, L/H or L/W. In this paper, the impact of different morphological scenarios for GEO variation on external ventilation levels within a typical high-rise Housing and Development Board (HDB) residential estate (or precinct) in Singapore, is analyzed through a parametric study exercise. The GEO values are quantified by using the author-proposed Maximum Hydraulic Diameter (HD_{Max}). Two types of common high-rise HDB block types are examined – point and slab blocks, in two types of configurations: (i) geometrical height variation and (ii) geometrical width variation. Numerical studies are done by utilizing a commercial computational fluid dynamics (CFD) code named Star-CCM+. External ventilation levels are quantified by using the area-averaged Wind Velocity Ratio (V_R) index, an indication of the average outdoor ventilation potential within an estate at a certain level above ground. Measurements were taken at both the pedestrian and mid-levels under different wind orientations. The final results indicated that in general, GEO is *positively* related to V_R and concluded the usefulness of using HD_{Max} instead of the common aspect ratios of canyons proposed by previous researchers, of which the scale and absolute size were not reflected and produced different gradients of relationship with V_R under different geometry range values. Case studies were also included at the later part of this paper to verify this positive relationship between GEO and V_R.**

Keywords- Canyon Geometry; Morphological Variables; Wind Velocity Ratio (V_R); Outdoor Ventilation; High-Rise Residential Estate; Parametric Study; Computational Fluid Dynamics (CFD)

I. INTRODUCTION

Many environmental problems such as higher air temperatures, high pollution levels and lower wind flow rates, are due to large-scaled urbanization. One of the by-products of urbanization is the unstructured and improper planning of urban morphologies and this causes the wind speed to seriously decrease by virtue of the buildings' roughness and geometry within [1]. Urban canyons' climate is primarily controlled by the micrometeorological effects of canyon geometry, rather than the mesoscale forces that control the urban boundary layer (UBL) climatic systems [2]. Many studies which involved field experiments, wind tunnel simulations and computational fluid dynamics (CFD) modeling had been done before. Their results have shown us that different near-surface wind flow regimes can result from the way urban morphologies are structured.

Based on literature review, the seven morphological variables that determine and have an association with natural outdoor ventilation within a high-rise residential precinct are Orientation [3-5], Building Shape [6], Gross Building Coverage Ratio [5, 7-12], Geometry [11, 13-15] Permeability [3, 7], Buildings' Height Variation [5, 16, 17] and Staggering of Blocks Arrangement [5, 12, 18, 19]. These studies by previous researchers postulate that there is an association between different morphological variables and outdoor ventilation potential. This paper will focus on a detailed parametric study on the effects of one of them - Geometry (GEO), on external ventilation levels within a typical high-rise Housing and Development Board (HDB) public residential estate (or precinct) in Singapore.

The term urban canyon can be explained as a relatively narrow street with buildings lined up continuously along both sides [20] (Fig. 1). Generally, dimensions of a street canyon are usually expressed by its aspect ratio, which is the height (H) of the canyon divided by the width (W) or H/W. The length (L) usually expresses the road distance between two major intersections, subdividing street canyons into short (L/H~3), medium (L/H~5), and long canyons (L/H~7). Urban streets might be also classified into symmetric (or even) canyons, if the buildings flanking both sides are approximately the same height, or asymmetric, if there are significant differences in building height [21].

Characteristics canyon geometries, expressed in terms of height-to-width (H/W) and length-to-height (L/H) ratios, are known to produce three principal air flow regimes when the above-roof wind direction is perpendicular to the canyon (approximately ±30° normal to the long axis of the street canyon): 'isolated roughness flow (IRF)', 'wake interference flow (WIF)' and 'skimming flow (SF)' [11, 13, 14] (Fig. 2). The mechanisms determining the flow characteristics in canyon are either the creation of a circulatory vortex due to momentum transfer across a shear layer at roof height, or the finite length canyon effects (end effects) that are related to intermittent vortices shed at building corners and responsible for the mechanism of advection from building corners to mid-block - creating a convergence zone in mid-block region [22-24]. Yamartino and

Wiegand reported that when L/W value decreases and reach approximately 20, finite-length canyon effects begin to dominate over the vortex [22], whereby flow characteristics become more three-dimension in nature [25, 26]. The street canyon aspect ratio H/W is the most important factor that not only influences the flow regimes (SF, WIF and IRF) but also characterizes different flow patterns *within the same* flow regime. E.g. the SF regime, which is widely studied, has also different numbers of re-circulations depending on H/W [27]. Furthermore, canopy length (L) governs the degree of interaction between the corner and cavity vortex near the edges of the street canyon. This may affect the flow regime transitions inside the same street canyon as well [2, 16].

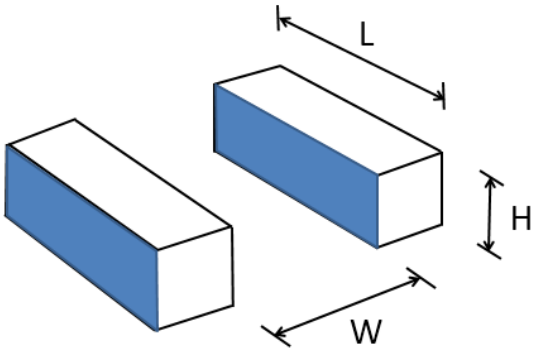

Fig. 1 General parameters for describing an urban canyon

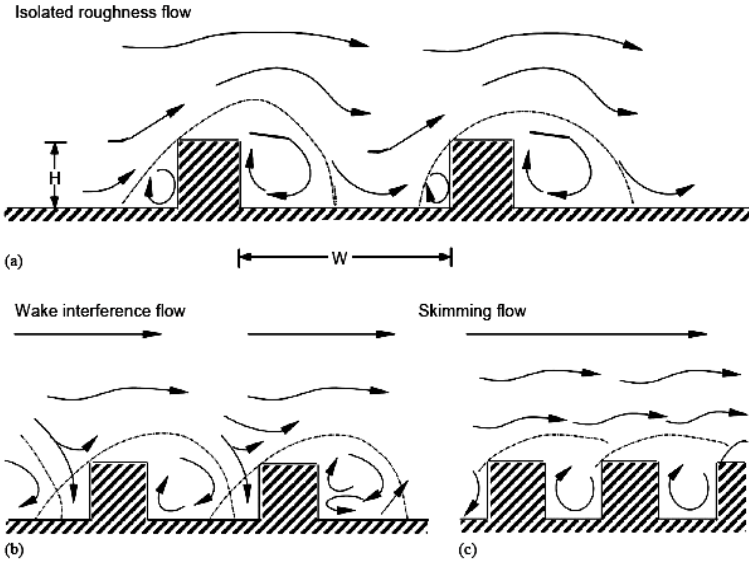

Fig. 2 Perpendicular flow regimes in urban canyons for different aspect ratios [11, 14]

The main problem of the above-mentioned ratios stems from the fact that they are based on numbers that do not actually reflect the actual scale of the canyons or buildings. For example, a symmetrical canyon of height (H) 20cm and width (W) 10cm will have the same H/W of two as another one with a height of 20m and a width of 10m. Next, in Chan et al.'s research, the three aspect ratios that were investigated are relative height of downwind and upwind H2/H1, H/W and L/W against the maximum pollutant concentration which is a proxy of ventilation level inside the canyon and exchange between in and out canyon air [16]. The progressive magnitude increase of these ratios does not produce a constant gradient of change where any behavioral conclusions can be made. Hence, in order to solve this problem, the author had come up with an index to quantify GEO which is called the Maximum Hydraulic Diameter (HD_{Max}). The details about this index will be described in the following sections.

A comprehensive parametric numerical study was carried out in order to study the association of GEO (quantified in the index form of HD_{Max}) with the area-averaged Wind Velocity Ratio (V_R) index, an indication of the average outdoor ventilation potential within an estate at a certain level above ground. A numerical simulation study in three-dimension, using the Reynolds-averaged Navier-Stokes (RANS) Realizable k-ε turbulence model (RLZ) by a commercial computational fluid dynamics (CFD) code, was used to study the impact of different morphological scenarios of GEO variation. The accuracy of this code by the name of Star-CCM+, has been validated by a comprehensive wind tunnel test, which was carried out in an open circuit boundary-layer wind tunnel (BLWT) at the National University of Singapore (NUS) and both the experimental and simulated results agree reasonably well [28]. Two types of common HDB block types in Singapore were examined – point and slab blocks, in two types of GEO configurations: (i) geometrical height variation and (ii) geometrical width variation, at

both the pedestrian and mid-levels under different wind orientations. At the later part of this paper, a few case studies which consist of a base HDB precinct plan proposal and two alternative variations from the base proposal, are used to demonstrate the usefulness of the Maximum Hydraulic Diameter (HD_{Max}) in quantifying the geometry of urban morphologies.

The objective of this present work is to investigate how the magnitude of outdoor ventilation within a precinct, vary with the GEO values. The methodology adopted and the results obtained will be discussed in detail in the following sections.

II. METHODOLOGY

An in-depth parametric study approach is adopted in this paper for the investigation of GEO on average outdoor ventilation within a said precinct. Numerical study is employed to simulate the conditions of a typical public HDB high-rise residential housing estate, which is set to a typical estate (precinct) size of approximately 500m×500m as the base case standard. The area-averaged outdoor velocity magnitude values will be extracted at the pedestrian level (cut at a constrained horizontal plane at 2m above ground, within the precinct) and mid-level (Fig. 3). The mid-levels will be fixed at 56m and 25m above ground for point and slab blocks respectively. These levels are according to the mid horizontal level of the average height of all buildings within the precinct for the *base cases* of the respective block types. These levels will be used throughout for extracting the outdoor average velocities. Outdoor velocity magnitude readings from all the cells within the highlighted box for the studied level are area-averaged (according to cell size) over the total area of all cells (within the highlighted box) at the same level.

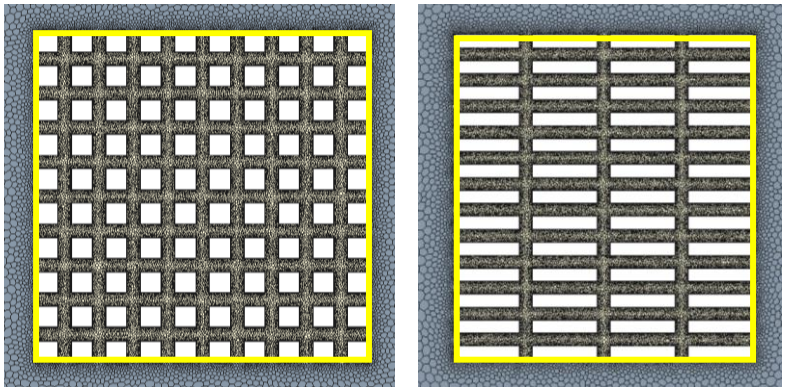

Fig. 3 Point (L) and slab (R) blocks layout in a 500×500m HDB estate – Readings from all the mesh cells within the highlighted yellow box (for studied level) are extracted and each area-averaged over the total area of all cells (within the highlighted box) for outdoor wind velocity magnitude

There are mainly two common physical forms of HDB block designs – point block and slab block. The design principles and precinct planning of HDB flats and their estates have been documented and described in detail by Lee et al. whereby the block design is very much affected by the flat unit type and mix, site planning consideration, number of units per block, height restriction within the area, population, demographics, etc. [28].

A. GEO Values and Configuration Types

For comparison purposes, two base case scenarios are used here, one for the **point blocks** (each block dimension is 30L×30W×112H metres) and another for **slab blocks** (each block dimension is 100L×20W×50H metres) whereby both are the most commonly adopted building shapes in Singapore [28, 30]. The base case spacing between the blocks is 20m apart. All the blocks are confined within a 500×500m HDB estate, assumed to be the maximum size we have for high density living in Singapore, given the current regulations and control.

Geometry variations in terms of building height (H) and width spacing (W) are being studied for both types of point and slab blocks for their effects in area-averaged V_R at the pedestrian and mid-levels. This study includes two types of variations:

- Varying the height (H) of all point blocks (from base case of 112m) and slab blocks (from base case of 50m).
- Varying the spacing (W) between all the blocks (from base case of 20m).

Note: For geometric width variation (W) cases, the boundary of the constraint plane will follow the outline perimeter of the whole precinct that is only inclusive of all the buildings' footprint and canyon areas combined within (similar to what we have done in the base case), instead of following the base case's size of 500m by 500m. The importance is to account for all buildings and canyons site coverage *only* regardless of their width variation.

The morphological index that is used to quantify Geometry (GEO) is the Maximum Hydraulic Diameter (HD_{Max}), which is defined as the summation of all the largest hydraulic diameter (HD) of individual outdoor grid space, that are each area-weighted over the whole given precinct. The HD_{Max} can be worked out using the following relation:

$$\mathbf{HD_{Max} = \Sigma\ [(Largest\ HD\ of\ Area\ \textit{i})*(\%\ of\ Area\ \textit{i}\ in\ Precinct)]}$$

HD is the hydraulic diameter of the studied area HD = 2HW/ (H+W) found within the precinct, where H = average height (metres) of both the upwind (H1) and downwind (H2) buildings on both sides of an open space or canyon, W = horizontal distance (or canyon width) between the buildings (metres) (Fig. 4). The researchers in Los Alamos National Laboratory attempted to use the same principle to map out the composite height-to-width ratio (instead of HD) for a residential precinct in Phoenix at the individual grid areas [29] (Fig. 5).

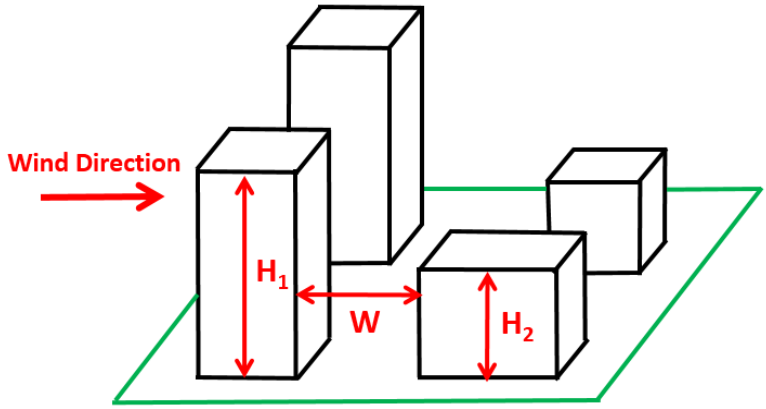

Fig. 4 Illustration of the different geometric parameters where, H1 = height of upwind building, H2 = height of downwind building and W = horizontal distance between both buildings

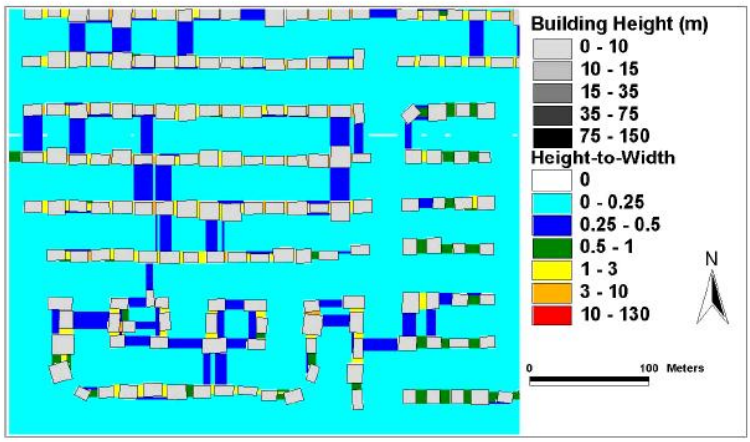

Fig. 5 Illustration of the composite height-to-width ratio for a residential section of a study area in Phoenix [29]

The calculation of HD is performed along linear traverses across the precinct at different angles for each pair of adjacent elements in a building array, of which the largest HD value is selected. This can be quite tedious for complex building shapes and pattern cases. The composite values of HD are computed at each grid area by selecting the largest value from the superimposed matrices from the two traversal directions. The HD_{Max} is computed by using the summation of area-weighted average of the spatial distribution of the largest composite HD value from each grid area. With this approach, buildings with larger footprints will exert a greater influence over the area-weighted average. In addition, open areas and street intersections will be calculated by using H as the average height of all the buildings within the estate and W is the largest dimension of the whole estate (e.g. 500m for base case) to work out the HD value.

The Geometry (GEO) values, derived from the HD_{Max}, used in this parametric study are as shown in Tables 1 and 2 for both the point and slab blocks study respectively. Variation cases that are highlighted in gray are not included in the parametric study for mid-levels as the building heights used are smaller than the mid-height values of 56m for point blocks and 25m for slab blocks.

Please note that in this parametric study, due to the ordered arrangement of the blocks, there are no areas that are subjected to more than one HD_{Max} (Fig. 6). But in the study of all the other morphological indices by the author, e.g. building shape, gross building coverage ratio [28], buildings' height variation [30] and staggering of blocks' arrangement, there would be cases that warrant the same individual area within the precinct to have more than one HD. For the study of other morphological variables, the GEO values (HD_{Max}) will also be mapped together with their own individual indices e.g. Gross Building Coverage Ratio (GBCR) for quantifying the ratio between ground area covered by buildings over the area of whole precinct [28], and Buildings' Height Variation (HV) index for quantifying the standard deviation of the height variation for all the high-rise buildings within the precinct [30].

TABLE 1 TABULATED VALUES OF POINT BLOCKS GEOMETRY (GEO) FOR THE PARAMETRIC STUDY

POINT BLOCKS (Height varies)

Case	Description	Height (m)	Width (m)	GEO
1	Point Blocks - HeightWidth - 15m, 20m	15.00	20.00	21.04
2	Point Blocks - HeightWidth - 35m, 20m	35.00	20.00	38.44
3	Point Blocks - HeightWidth - 55m, 20m	55.00	20.00	52.01
4	Point Blocks - HeightWidth - 75m, 20m	75.00	20.00	63.71
5	Point Blocks - HeightWidth - 95m, 20m	95.00	20.00	74.20
6	Point Blocks - BASE	112.00	20.00	82.39
7	Point Blocks - HeightWidth - 125m, 20m	125.00	20.00	88.28
8	Point Blocks - HeightWidth - 145m, 20m	145.00	20.00	96.79
9	Point Blocks - HeightWidth - 165m, 20m	165.00	20.00	104.72
10	Point Blocks - HeightWidth - 185m, 20m	185.00	20.00	112.14
11	Point Blocks - HeightWidth - 205m, 20m	205.00	20.00	119.10

POINT BLOCKS (Width varies)

Case	Description	Height (m)	Width (m)	GEO
1	Point Blocks - HeightWidth - 112m, 5m	112.00	5.00	20.70
2	Point Blocks - HeightWidth - 112m, 10m	112.00	10.00	38.66
3	Point Blocks - HeightWidth - 112m, 15m	112.00	15.00	54.32
4	Point Blocks - HeightWidth - 112m, 25m	112.00	25.00	80.08
5	Point Blocks - BASE	112.00	20.00	82.39
6	Point Blocks - HeightWidth - 112m, 30m	112.00	30.00	90.74
7	Point Blocks - HeightWidth - 112m, 35m	112.00	35.00	100.21
8	Point Blocks - HeightWidth - 112m, 40m	112.00	40.00	108.66

TABLE 2 TABULATED VALUES OF SLAB BLOCKS GEOMETRY (GEO) FOR THE PARAMETRIC STUDY

SLAB BLOCKS (Height varies)

Case	Description	Height (m)	Width (m)	GEO
1	Slab Blocks - HeightWidth - 10m, 20m	10.00	20.00	14.81
2	Slab Blocks - HeightWidth - 20m, 20m	20.00	20.00	24.35
3	Slab Blocks - HeightWidth - 30m, 20m	30.00	20.00	31.68
4	Slab Blocks - HeightWidth - 40m, 20m	40.00	20.00	37.84
5	Slab Blocks - BASE	50.00	20.00	43.26
6	Slab Blocks - HeightWidth - 60m, 20m	60.00	20.00	48.18
7	Slab Blocks - HeightWidth - 70m, 20m	70.00	20.00	52.72
8	Slab Blocks - HeightWidth - 80m, 20m	80.00	20.00	56.96
9	Slab Blocks - HeightWidth - 90m, 20m	90.00	20.00	60.96

SLAB BLOCKS (Width varies)

Case	Description	Height (m)	Width (m)	GEO
1	Slab Blocks - HeightWidth - 50m, 5m	50.00	5.00	11.60
2	Slab Blocks - HeightWidth - 50m, 10m	50.00	10.00	21.09
3	Slab Blocks - HeightWidth - 50m, 15m	50.00	15.00	28.97
4	Slab Blocks - HeightWidth - 50m, 25m	50.00	25.00	41.45
5	Slab Blocks - BASE	50.00	20.00	43.26
6	Slab Blocks - HeightWidth - 50m, 30m	50.00	30.00	46.42
7	Slab Blocks - HeightWidth - 50m, 35m	50.00	35.00	50.75
8	Slab Blocks - HeightWidth - 50m, 40m	50.00	40.00	54.54

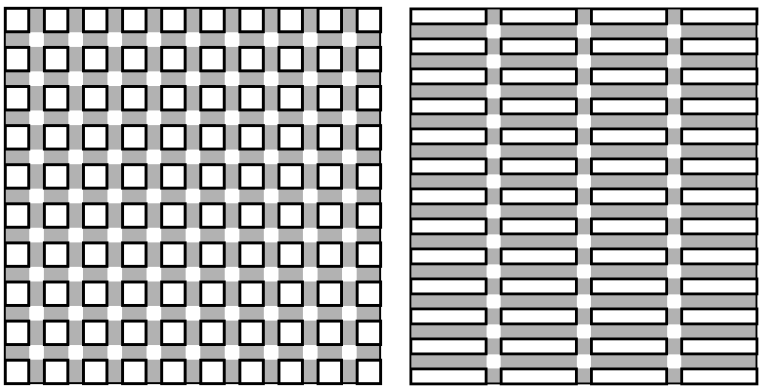

Fig. 6 Shaded areas showing the composite HD_{Max} for the HDB precinct area for both point (left) and slab blocks (right)

B. Numerical Simulations

The Realizable *k-ε* turbulence model (RLZ), one of the RANS model variants, is selected for use in the simulation studies of this research. This is a revised *k-ε* turbulence model proposed by Shih et al. [31]. Solutions to the problem here utilized this turbulent model whereby the Navier-Stokes equations are discretized using a finite volume method. The SIMPLE algorithm is used to handle the pressure-velocity coupling and the following set of discretized algebraic equations is solved by the segregated method.

The four types of partial differential equations that need to be solved are [31, 32]:

(1) Continuity equation

$$\frac{\partial u_j}{\partial x_j} = 0$$

(2) RANS equations (in x, y and z directions)

$$\frac{\partial u_i}{\partial t} + u_j \frac{\partial u_i}{\partial x_j} = -\frac{1}{\rho}\frac{\partial P}{\partial x_i} + \frac{\mu}{\rho}\frac{\partial^2 u_i}{\partial x_j \partial x_j} - \frac{\partial}{\partial x_j}(\overline{u_i' u_j'}) + g_i$$

Two turbulence closure equations for realizable k-ε (RLZ):

(3) Turbulent kinetic energy (k) (m^2s^{-2})

$$\frac{\partial k}{\partial t} + u_j \frac{\partial k}{\partial x_j} = \frac{1}{\rho}\frac{\partial}{\partial x_j}\left[\left(\mu + \frac{\mu_t}{\sigma_k}\right)\frac{\partial k}{\partial x_j}\right] + \frac{G_k}{\rho} - \varepsilon$$

(4) Dissipation rate of turbulent kinetic energy (ε) (m^2s^{-3})

$$\frac{\partial \varepsilon}{\partial t} + u_j \frac{\partial \varepsilon}{\partial x_j} = \frac{1}{\rho}\frac{\partial}{\partial x_j}\left[\left(\mu + \frac{\mu_t}{\sigma_\varepsilon}\right)\frac{\partial \varepsilon}{\partial x_j}\right] + C_1 S\varepsilon - C_2 \frac{\varepsilon^2}{k + \sqrt{\nu\varepsilon}}$$

The Reynolds stress is:

$-(\overline{u_i' u_j'}) = \frac{1}{\rho}\mu_t\left(\frac{\partial u_i}{\partial x_j} + \frac{\partial u_j}{\partial x_i}\right) - \frac{2}{3}k\delta_{ij}$, where $\mu_t = \rho\frac{C_\mu k^2}{\varepsilon}$ is the turbulent viscosity; where C_μ is a model constant which is not fixed.

$$C_\mu = \frac{1}{A_0 + A_S(kU^*/\varepsilon)}, \text{ where } A_0 = 4.04,$$

$$A_s = \sqrt{6}\cos\phi,$$

$$\phi = \frac{1}{3}\left(\cos^{-1}\left(\sqrt{6}W\right)\right),$$

$$W = S_{ij}S_{jk}S_{ki}/\tilde{S}^3,$$

$$\tilde{S} = \sqrt{S_{ij}S_{ij}},$$

$$S_{ij} = \frac{1}{2}\left(\left(\partial u_j/\partial x_i\right) + \left(\partial u_i/\partial x_j\right)\right),$$

$U^* = \tilde{S} = \sqrt{S_{ij}S_{ij}}$ (Where there is no rate of rotation in the stationary reference frame for this study).

Legend:

u_j = *j* component of *mean* velocity (ms^{-1});

u_j' = root-mean-square of the velocity fluctuation *j* component;

P = pressure in Newton per meter square (Nm^{-2});

t = time in seconds (s);

x_j = j coordinate (m);

ρ = air density (kgm^{-3});

μ = dynamic (molecular) viscosity ($kgm^{-1}s^{-1}$);

g_i = gravitational body force (ms^{-2});

G_k = turbulent kinetic energy production ($kgm^{-1}s^{-2}$);

S = scalar measure of deformation or mean strain rate (m^2s^{-2});

ν = molecular kinematic viscosity (μ/ρ);

Constants:

σ_k = 1.0 (Turbulent Prandtl number for k);

σ_ε = 1.2 (Turbulent Prandtl number for ε);

C_1 = $\max\left[0.43, \frac{\eta}{\eta+5}\right]$, where $\eta = Sk/\varepsilon$, where $S = \sqrt{2S_{ij}S_{ij}}$ is the scalar measure of the deformation tensor;

C_2 = 1.9.

The RLZ turbulence model performs best in separated flows and flows with complex secondary flow, provided that it is properly coupled with a two-layer all y^+ wall treatment near the 'wall' boundary condition [31, 33, 34]. Furthermore, this model has also shown superiority in modeling flows that include boundary layers under strong adverse pressure gradients, separation and recirculation as compared to others RANS models [31, 34] and excels at modeling flows that involved high shear or separation commonly encountered in building simulation [35]. All the simulation cases are carried out under steady state fluid flow and isothermal conditions. Air within the domain is regarded as incompressible turbulent inert flow which is according to the assumption that at low subsonic speeds, air densities are considered constant under varying pressures at lower atmospheric environment as described by Sini et al. [15].

C. Computational Domain and Mesh Type

The computational domain adopted here consists of a large cylindrical atmospheric volume of radius 1800m and height of 800m, similar to the one proposed by Lee et al. as shown in Fig. 7 [28, 30]. The middle portion of this atmospheric domain consists of the HDB blocks whereby the parametric study of morphological variations will be carried out. The domain radius is 3 times of the longest distance length of the development from the development boundary to the domain edge [36]. The domain height extends 6 times the tallest building's height from the top of the highest building in the whole development to the top of the domain [37]. We used the height of the point blocks (112m), which are taller compared to the slab blocks (50m). Both requirements are the most stringent among those suggested by most researchers and guidelines.

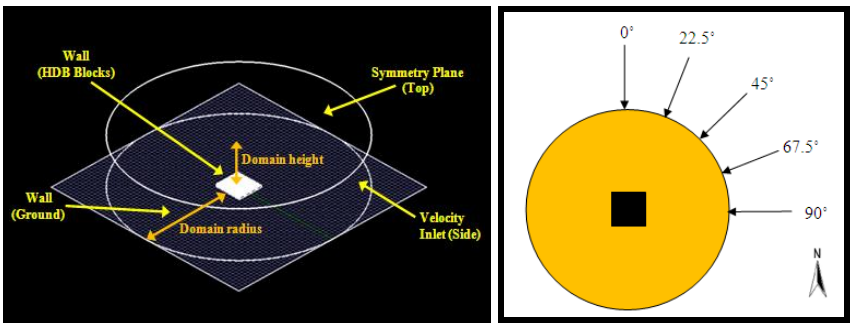

Fig. 7 Computational domain and wind orientations from north; the middle estate area of 500×500m will be subjected to various morphological variations [28, 30]

Unstructured polyhedral grids with a growth factor of 0.9 are generated for the whole computational domain. A mesh independence test that was done by Lee et al., whereby a localized mesh size of 1.5m for the HDB blocks does not show any further changes in simulation results with further decrease in mesh size [30]. Hence, a localized mesh size of 1.5m or less can be used and the size chosen for all simulations is 1.2m. Wind from different orientations will be simulated with the same cylindrical domain (Fig. 7). The curved inlet boundary acts as the inflow of winds from different orientations (0°, 22.5°, 45°, 67.5° and 90° north). The cylindrical top is a symmetry plane (slip wall condition) and the cylinder bottom (non-slip wall

condition) is where the power-law wind profile will move in from the inlet before arriving at the estate area. The outlet is considered to be the opposite side of the wind orientation.

D. Boundary Conditions

A power-law wind profile is generated (using BCA's Code for Environmental Sustainability of Buildings, 2nd Edition), averaged at 2.7m/s from all the four prevailing wind directions (at reference height of 15.00m) [36] (Table 3). The other input variables are as shown in Table 4.

TABLE 3 TABULATION OF PREVAILING WIND DIRECTION AND SPEED OBTAINED FROM NEA (NATIONAL ENVIRONMENT AGENCY) OVER A PERIOD OF 18 YEARS [36]

Wind Direction	Mean Speed (m/s)
North	2.0
North-east	2.9
South	2.8
South-east	3.2

TABLE 4 INPUT VARIABLES FOR THE INLET BOUNDARY CONDITIONS [28, 30]

Parameter	Value	Input	Researcher
Power law exponent (α)	α = 0.21 [38].	Power law – to approximate the vertical upwind profile flow in medium density suburban areas. Ensuring that the minimum threshold speeds of 2m/s (ambient wind for above-roof) for development of canyon vortices observed by DePaul and Shieh was comfortably exceeded.	De Paul and Shieh, 1986 [40]
Roughness length (Z_0)	Z_0 = 0.5 (Suburban terrains, forest, regular large obstacles, etc). [39]		
Turbulence intensity (Ti)	5% (low speed flows for ventilation)		
Turbulent kinetic energy (*k*)	At Ti =5%, occurs at H = 467m above ground of the power-law wind profile worked out. Wind velocity at this height is Ur = 5.56m/s [38].	$k = \frac{3}{2}(U_r T_i)^2$ Where Ti represents the turbulence intensity, Ur is the reference velocity at the level where Ti = 5%.	
Turbulent dissipation (ε)		$\varepsilon = \frac{C_\mu^{3/4} k^{3/2}}{l}$ Empirical constant Cμ = 0.09 and l = 0.07L, where L is the characteristic length and in this case, the longest distance measured across each estate. I.e. the length of the estate = 500m.	
Von Karman constant	K = 0.41 (urban areas)		

E. Wind Velocity Ratio (V_R)

The wind velocity ratio (V_R) is used as an indicator of good ventilation in this study. It is measured and defined as $V_R = V_p / V_\infty$, where V_∞ is the wind velocity at the top of an UBL not affected by the ground roughness, buildings and local site features (typically assumed to be at a certain height above the roof tops of the area and is site dependent) [41]. V_P is the wind velocity at pedestrian level (2m above ground) after taking into account the effects of buildings. V_R indicates how much of the wind availability of a location could be experienced by pedestrians near the ground taking into account the surrounding buildings. The concept of V_R can also be used for other measured levels besides pedestrian level.

Lee et al. mentioned that according to the incoming Singapore power-law wind profile as mentioned in the section on 'Boundary Conditions', V_∞ will be fixed (for all V_R calculations) at a certain height above ground [28, 30]. This height level is where the change in incoming wind velocity between the selected level (1m interval between each level) and the cylindrical domain top that is assumed to be at 800m above ground has a difference of 1% or less. It was worked out that according to the wind profile of α = 0.21 where the top of the cylindrical domain at 800m above ground, yields a wind speed of 6.22m/s. At 745m above ground, we obtained a speed of 6.13m/s which is about 1% difference between it and the wind speed at 800m above ground. Hence, V_∞ as 6.13m/s is used for working out the V_R.

The area-averaged outdoor velocity magnitude values for V_P will be extracted at the pedestrian-level (2m above ground level) and the mid-level (56m for point blocks and 25m for slab blocks) and area-averaged (according to cell size) within a constrained horizontal plane that is confined within the precinct area.

III. RESULTS AND DISCUSSIONS

A. Point Blocks, Pedestrian Level

The overall results for area-averaged V_R values within the estate for point blocks under the geometrical height variation (H) and geometrical width variation (W) GEO configurations are shown in Fig. 8 for the pedestrian level.

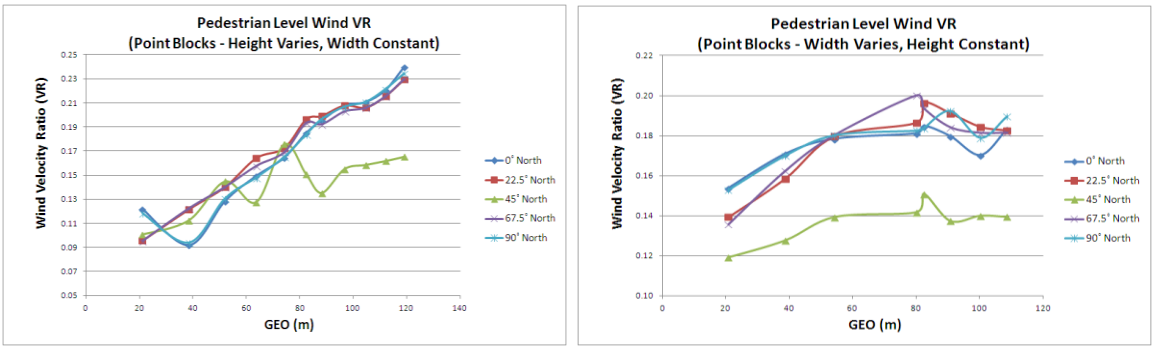

(a) (b)

Fig. 8 Pedestrian level area-averaged V_R against GEO for (a) geometric height variation (H) and (b) geometric width variation (W) configurations of point blocks

1) Point Blocks, Pedestrian Level – Geometrical Height Variation (H):

V_R readings for all the wind orientations increase steadily as GEO increases (Fig. 8a). But for winds from 45 ° north orientation, the gradient and magnitude of V_R increase is not as high as other wind orientations. Generally, the increase in V_R at the pedestrian level is due to the increase in channeling effects accorded to a suitable canyon width (that is not too narrow) for the ranges of geometric height variation (H) increase here. For orientations that are parallel or oblique to the wind direction (0˚, 22.5˚, 67.5˚ and 90˚ north), their higher magnitudes and gradient of increase are due to the higher degree of channeling effects. For example, in Figs. 9a and 9b, we can see the increase in channeling phenomena for 0˚ north wind orientation when the height of the point blocks increases from 35m to 185m, respectively.

The lower gradient and magnitude of increase for 45˚ north wind is due to the inflow from both directions of the transverse main canyons which provide opposing flows that slow down the overall outdoor wind relative to other orientations. In Figs. 9c and 9d, we can see the increase in channeling phenomena for 45˚ north wind orientation when the height of the point blocks increases from 35m to 185m, respectively. But the magnitude and gradient of increase is not as significant as the other orientations at the same level.

Next, V_R readings for wind orientations 0˚, 22.5˚, 67.5˚ and 90˚ north are closer to each other. This is because, for a point block precinct, it has more symmetrical dimensions (four equal sides) with similar number of urban canyons at both transverse orientations (0˚ and 90˚ north). Wind flows for these four orientations have more channeling effects and are less opposing, unlike those from 45˚ north. The second possibility is that pedestrian level winds are much more laminar and less turbulent than higher levels; hence there are steadier and less differences in V_R readings among these four orientations.

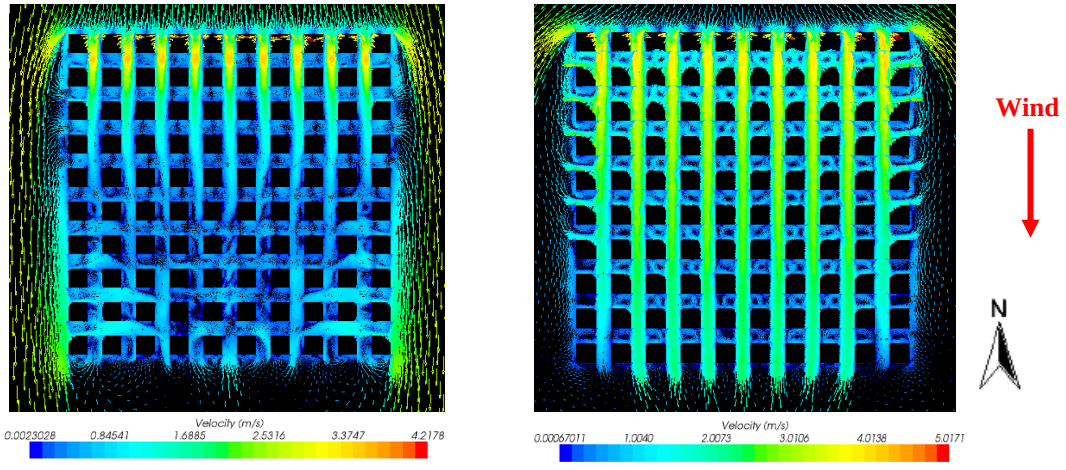

(a) (b)

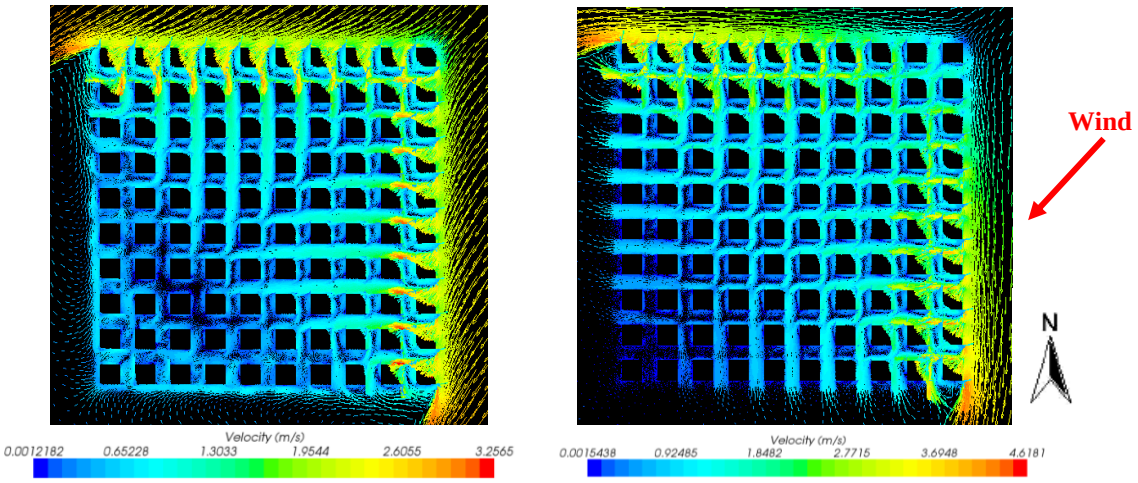

(c) (d)

Fig. 9 Point blocks, geometric height variation (H) configuration:

(a) Velocity vectors for GEO = 38.44 (35m height, 20m width) for wind from 0˚ north (pedestrian level), plan view
(b) Velocity vectors for GEO = 112.14 (185m height, 20m width) for wind from 0˚ north (pedestrian level), plan view
(c) Velocity vectors for GEO = 38.44 (35m height, 20m width) for wind from 45˚ north (pedestrian level), plan view
(d) Velocity vectors for GEO = 112.14 (185m height, 20m width) for wind from 45˚ north (pedestrian level), plan view

2) Point Blocks, Pedestrian Level – Geometrical Width Variation (W) Configuration:

V_R readings for all the wind orientations at pedestrian level increase steadily as GEO increases. But subsequently, the V_R values stop increasing and plateaus off. (Fig. 8b) Winds from 45˚ north orientation follows an almost similar behavioral pattern as the rest of the other orientations, except that their V_R are the lowest among all the orientations by a constant magnitude.

The initial V_R increase is basically due to the increase in wind flow from the increase in canyons width. It is different from the channeling effects as mentioned in the geometric height variation (H) configuration. For example, in Figs. 10a and 10b, we can see the increase in mass flow rate for 0˚ north wind orientation when the width between the point blocks increases from 5m to 25m, respectively (Figs. 10a and 10b). In the geometric width variation (W) configuration, the canyon width in the range from GEO = 20.70 (112m high, 5m width) to 80.08 (112m high, 25m width) is perceived to be too narrow to allow air to move in freely within the precinct, not to mention being able to benefit from any channeling effects; hence with an increase in canyon width leads to improved ventilation with higher mass flow rates. For 45˚ north wind orientation, the reason for their V_R magnitude lesser than the rest by a constant margin of about 0.04 is due to the inflow from both directions of the transverse main canyons which provides opposing flows that slows down the overall outdoor wind relative to other orientations which have a more straight-forward and unobstructed wind flow.

The continual increase in GEO will reach a point when V_R values for all wind orientations started to plateau from further GEO increase (increase in canyon width). Figs. 10c and 10d show the difference in flow patterns between GEO = 90.74 (112m height, 30m width) and GEO = 108.66 (112m height, 40m width) for 0˚ north wind orientation, respectively (Figs. 10c and 10d). Fig. 10e is an enlarged section view which shows quite similar flow pattern structures throughout the building heights for GEO = 90.74 (112m height, 30m width) and GEO = 108.66 (112m height, 40m width) where wind vortices are not so much ‘cramped’ by the narrowness of the canyons (Fig. 10e). It shows that canyon width increase has reached a threshold value whereby any further increase will not provide any further channeling effects nor significant increase in mass flow rate when their predominantly stabilized near wake-interference or isolated roughness wind flow structures at the upper levels has been attained. Another observation is that wind orientations for 0˚, 22.5˚, 67.5˚ and 90˚ north are closer to each other. The reasons are similar to Point Blocks, Pedestrian Level – Geometrical Height Variation (H) Configuration.

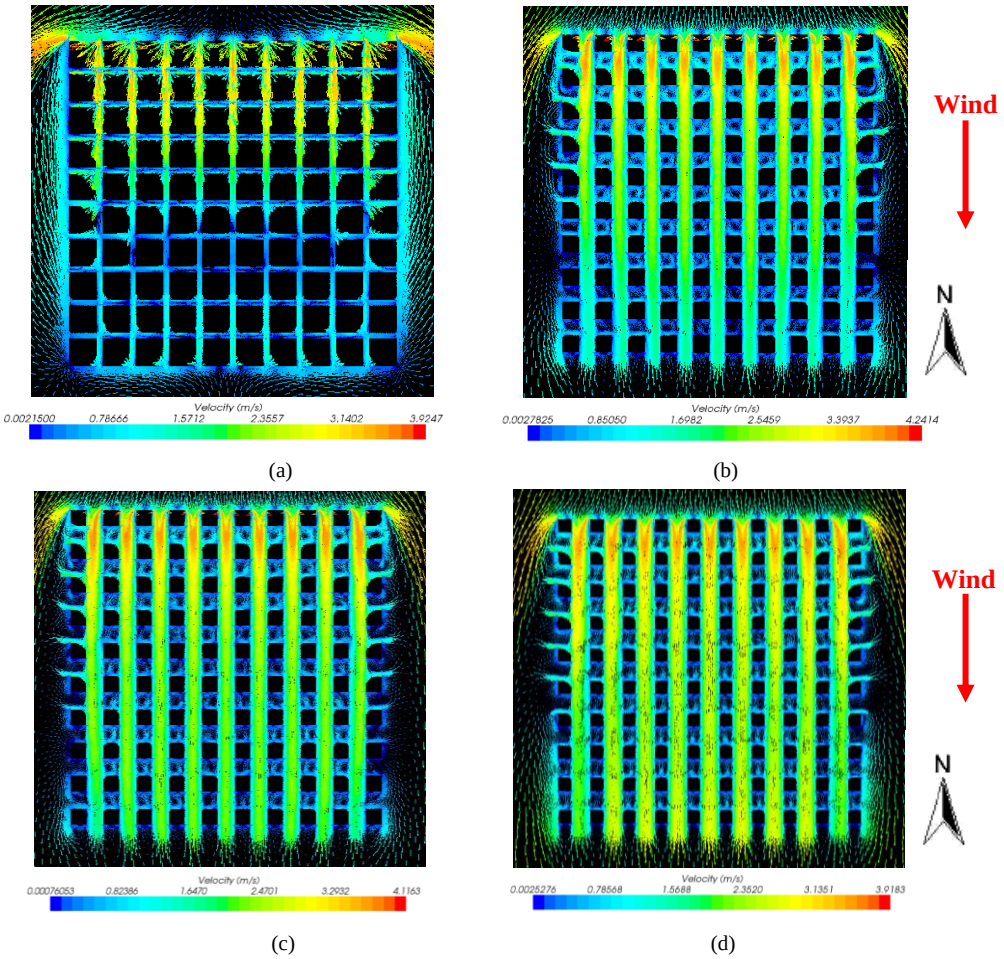

Fig. 10 Point blocks, geometric width variation (W) configuration:

(a) Velocity vectors for GEO = 20.70 (112m height, 5m width) for wind from 0˚ north (pedestrian level), plan view
(b) Velocity vectors for GEO = 80.08 (112m height, 25m width) for wind from 0˚ north (pedestrian level), plan view
(c) Velocity vectors for GEO = 90.74 (112m height, 30m width) for wind from 0˚ north (pedestrian level), plan view
(d) Velocity vectors for GEO = 108.66 (112m height, 40m width) for wind from 0˚ north (pedestrian level), plan view

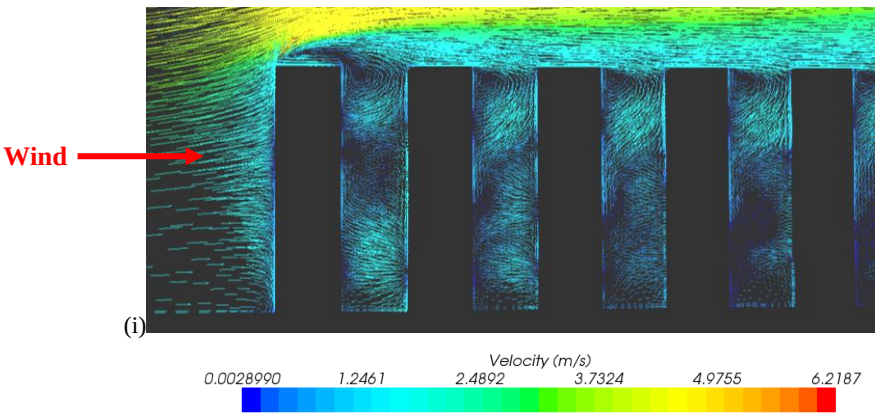

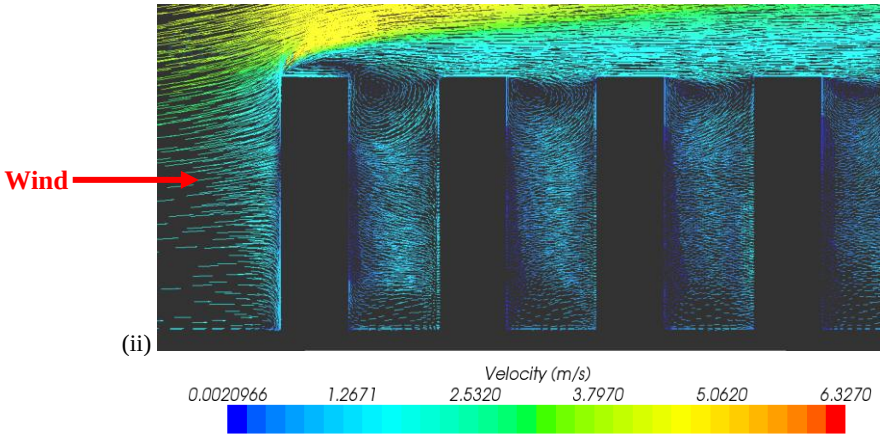

Fig. 10(e) Close-up view of point blocks, geometric width variation (W) configuration:

(i) Velocity vectors for GEO = 90.74 (112m height, 30m width) for wind from 0˚ north (pedestrian level), part section view
(ii) Velocity vectors for GEO = 108.66 (112m height, 40m width) for wind from 0˚ north (pedestrian level), part section view

B. Point Blocks, Mid-Level

The overall results for area-averaged V_R values within the estate for point blocks under the geometrical height variation (H) and geometrical width variation (W) GEO configurations are shown in Fig. 11 for the mid-level.

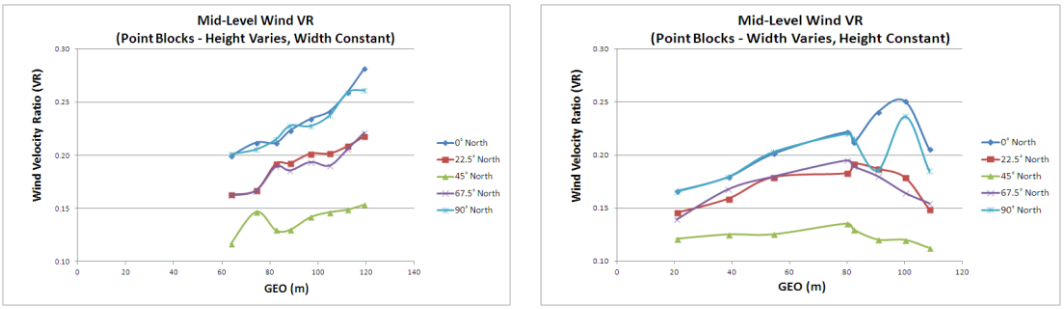

(a) (b)

Fig. 11 Mid-level area-averaged V_R against GEO for (a) geometric height variation (H) and (b) geometric width variation (W) configurations of point blocks

1) Point Blocks, Mid-Level – Geometrical Height Variation (H) Configuration:

In the geometric height variation (H) configuration for point blocks at mid-level, V_R increases steadily as GEO increases for all the wind orientations (Fig. 11a). The reason for the increase in V_R is the same as for Point Blocks, Pedestrian Level – Geometrical Height Variation (H) Configuration.

For wind orientations from 0˚ and 90˚ north, the mid-level V_R readings are higher than those at the pedestrian level (Figs. 8a and 11a). This is due to the power-law wind profile which comes in parallel to the main canyons and this allows the highest degree of channeling with wind being the stronger at higher levels. The magnitude of this channeling effect is most prominent in 0˚ and 90˚ north wind orientations, followed by 22.5˚ and 67.5˚ north orientations.

For the other wind orientations like 22.5˚ and 67.5˚ north, V_R readings for mid-levels are slightly lower than those at the pedestrian levels. For canyons that are oblique to the wind direction, winds tend to be more 'bent' and channeling effect is relatively not as strong as parallel orientations. This tends to cause more disturbances throughout different levels whereby the upper levels, with higher turbulence, will be more disturbed; hence their supposed higher wind speed becomes more disrupted and reduced than wind at pedestrian level (Fig. 12). For pedestrian levels, the wind flow is much more laminar and less turbulent than higher levels; hence wind flows from 22.5˚ and 67.5˚ north are steadier and do not differ much from those at 0˚ and 90˚ north orientations.

For wind orientation of 45˚ north, the reason for the lower gradient and magnitude of increase is the same as for Point Blocks, Pedestrian Level – Geometrical Height Variation (H) Configuration.

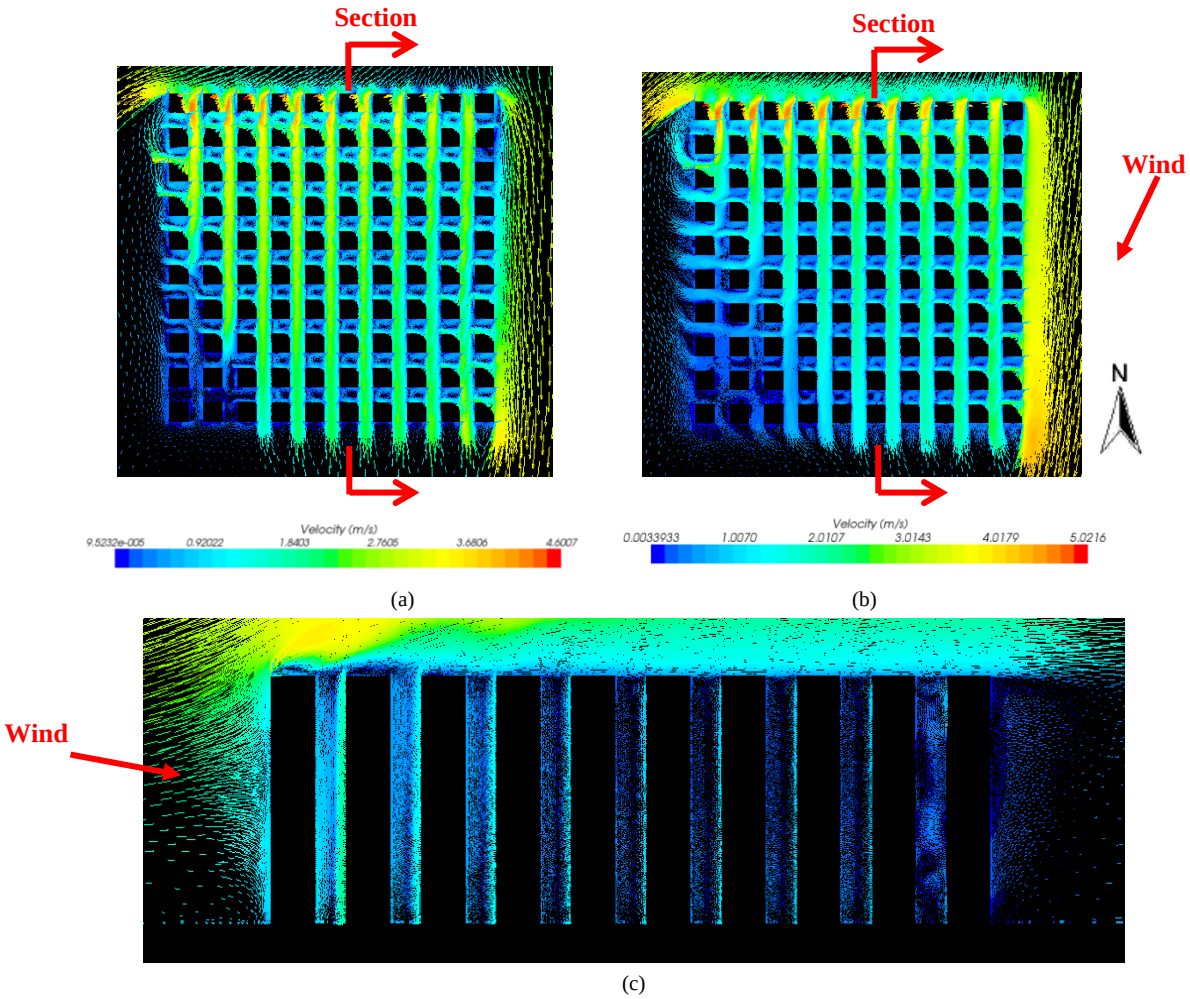

Fig. 12 Point blocks, geometric height variation (H) configuration – Velocity vectors for GEO = 104.72 (165m height, 20m width) for wind from 22.5 °north (a) Pedestrian level plan view; (b) Mid-level plan view; (c) Section view

2) Point Blocks, Mid-Level – Geometrical Width Variation (W) Configuration:

In the geometric width variation (W) configuration for point blocks at mid-level, V_R readings for all wind orientations increase steadily as GEO increases (Fig. 11b). But subsequently, the V_R readings stop increasing and start to become erratic. For 45˚ north wind orientation, the V_R magnitude is the lowest among the rest by a constant margin. The reasons behind these are the same as Point Blocks, Pedestrian Level – Geometrical Width Variation (W) Configuration.

The reason for the erratic V_R readings at the later part of GEO increase after 80.08 (112m high, 25m width), is due to the fact that canyon width increase has reached a threshold value whereby any further increase will not provide any increase in mass flow rate with their predominantly stabilized near wake-interference or isolated roughness wind flow structures at upper levels. Figs. 13a and 13b show the small difference in flow patterns between GEO = 90.74 (112m height, 30m width) and GEO = 108.66 (112m height, 40m width) for 0˚ north wind orientation (Figs. 13a and 13b).

For mid-level readings, V_R values for canyons that are parallel to the wind directions are higher than that of pedestrian level. Likewise for canyons that are oblique to wind direction, the mid-level V_R readings are lower than that of pedestrian level (Figs. 8b and 11b). The reasons are also similar to Point Blocks, Mid-Level – Geometrical Height Variation (H) Configuration.

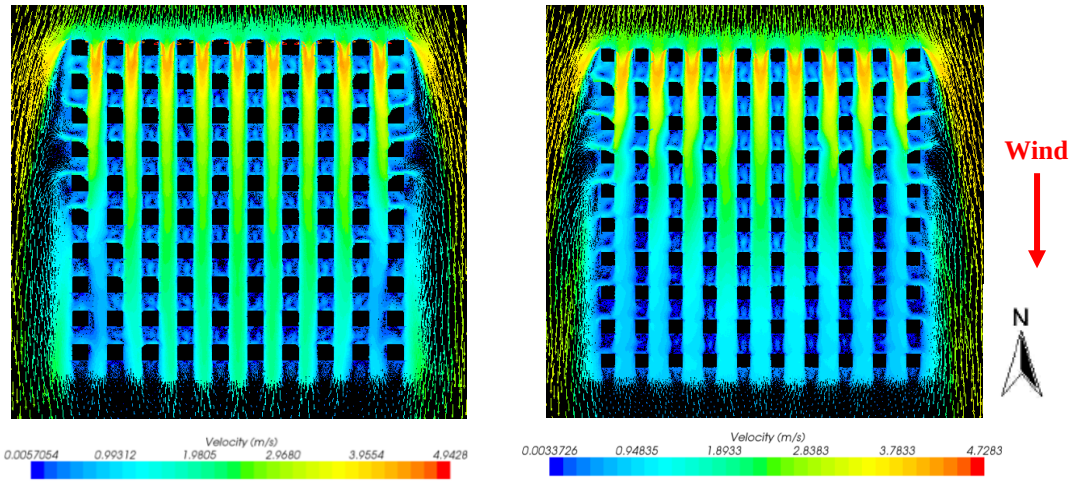

(a) (b)

Fig. 13 Point blocks, geometric width variation (W) configuration:

(a) Velocity vectors for GEO = 90.74 (112m height, 30m width) for wind from 0˚ north (mid-level), plan view
(b) Velocity vectors for GEO = 108.66 (112m height, 40m width) for wind from 0˚ north (mid-level), plan view

C. Point Blocks – Combined Results of Geometrical Height (H) and Width (W) Variation

Fig. 14 shows the combined results of GEO variations for both geometric height (H) and width (W) variation at pedestrian and mid-levels for point blocks. We can see that the overall V_R results show an increasing trend with increasing GEO variation.

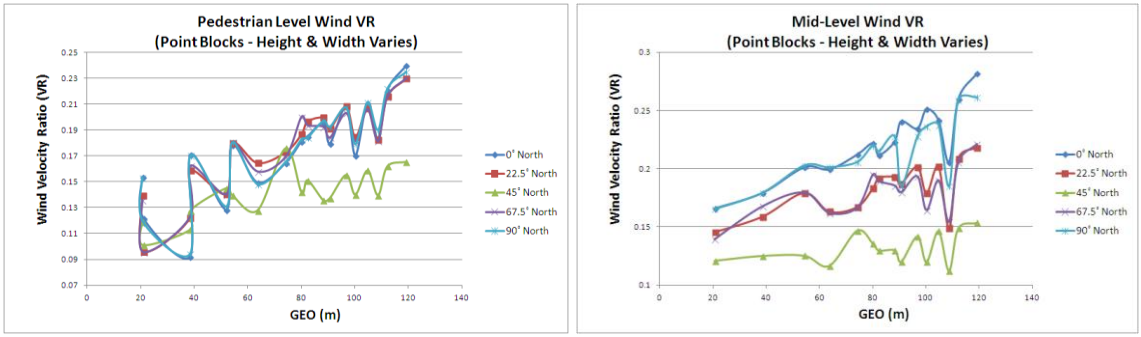

Fig. 14 Pedestrian and mid-levels area-averaged V_R against GEO for combined geometric height variation (H) and geometric width variation (W) configurations of point blocks

D. Slab Blocks, Pedestrian Level

The overall results for area-averaged V_R values within the estate for slab blocks under the geometrical height variation (H) and geometrical width variation (W) GEO configurations are shown in Fig. 15 for pedestrian level.

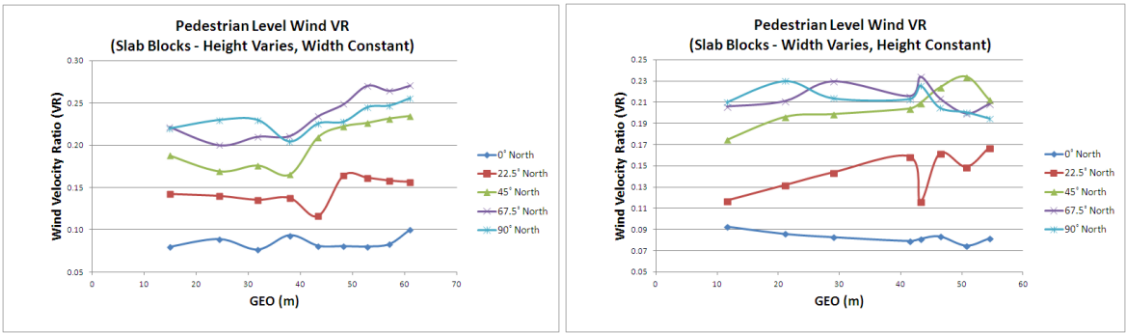

(a) (b)

Fig. 15 Pedestrian level area-averaged V_R against GEO for (a) geometric height variation (H) and (b) geometric width variation (W) configurations of slab blocks

1) Slab Blocks, Pedestrian Level – Geometrical Height Variation (H) Configuration:

V_R readings for all the wind orientations increase steadily as GEO increases (Fig. 15a). This V_R increase is due to the increase in channeling effects according to a suitable canyon width (that is not too narrow) for the ranges of geometric height variation (H) increase here. This effect is similar to the case for Point Blocks, Pedestrian Level – Geometrical Height Variation (H) Configuration.

The gradient of V_R increase gets progressively larger from 0˚ to 90˚ north wind orientation due to the progressive reduction in wall blockages. When there is higher number of blockages (e.g. 0˚ north orientation), the amount of wind entering a precinct will be very much reduced; hence V_R will still increase with an increase in GEO, but will be relatively slower compared to other orientations with more canyons parallel or oblique to the wind.

Next, the magnitude of V_R increases progressively from 0˚ to 90˚ wind orientations. The increase in V_R magnitude is due to the progressively higher degree of channeling effects when we move from 0˚ (lesser number of canyons oblique or parallel to it) to 90˚ north wind orientation (larger number of canyons oblique or parallel to it). Figs. 16a and 16b show the same height variation (H) configuration GEO = 48.18 (60m height, 20m width) for 0˚ and 90˚ wind orientation respectively, whereby the later shows higher wind flow into the precinct (Figs. 16a and 16b).

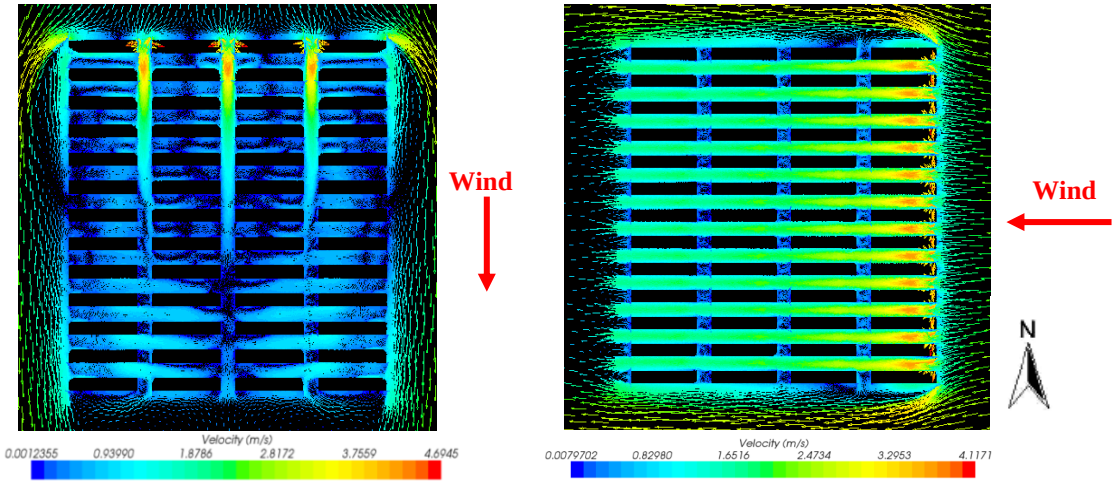

(a) (b)

Fig. 16 Slab blocks, geometric height variation (H) configuration:

(a) Velocity vectors for GEO = 48.18 (60m height, 20m width) for wind from 0˚ north (pedestrian level), plan view
(b) Velocity vectors for GEO = 48.18 (60m height, 20m width) for wind from 90˚ north (pedestrian level), plan view

2) Slab Blocks, Pedestrian Level – Geometrical Width Variation (W) Configuration:

V_R readings for all the wind orientations at pedestrian do not follow the same pattern with GEO increase (Fig. 15b). Their magnitudes and gradient of V_R increase against GEO depends on the number of canyons parallel or oblique to the wind direction which translated to the degree of channeling effects in play. The higher number of canyons also translates into less massive wall areas that cause wind blockages to ambient winds. All these will affect the gradient and magnitude of the V_R with progressive GEO increase.

For 0˚ north wind orientation, V_R readings have a slight decreasing trend throughout the range of GEO increase. The almost constant low V_R readings could be due to its highest level of blockage from the massive walls facing the wind from this direction. Since it has only three canyons parallel to the wind, channeling effects do not play a significant role in the variation of V_R values. For example, Fig. 17a shows GEO = 21.09 (50m height, 10m width) and Fig. 17b shows GEO = 46.42 (50m height, 30m width), both for 0˚ north orientation. The increase in width (increase in GEO) did not help to increase the value of V_R (Figs. 17a and 17b).

For both 22.5˚ and 45˚ north orientations, there are signs of increasing V_R values that come from the increase in GEO. The increasing V_R readings for 22.5˚ and 45˚ north orientations are due to higher mass flow rate that comes from the increase in canyon width. Unlike the point blocks, there is no threshold GEO value whereby V_R readings started to plateau or become erratic due to stabilization of vortex structures or increase in ground roughness. The reason is that for 22.5˚ and 45˚ north orientations, the massive wall surfaces that are facing 0˚ north still exert a strong negative influence over a wide range of GEO values which override the above-mentioned influences; hence any increase in canyon width continues to have a positive effect to the precinct's overall ventilation. Fig. 17c shows the wind flow for GEO = 21.09 (50m height, 10m width) and Fig. 17d shows GEO = 46.42 (50m height, 30m width), both for 22.5˚ north winds (Figs. 17c and 17d). We can see the increase in wind flow from GEO = 46.42 compared to GEO = 21.09.

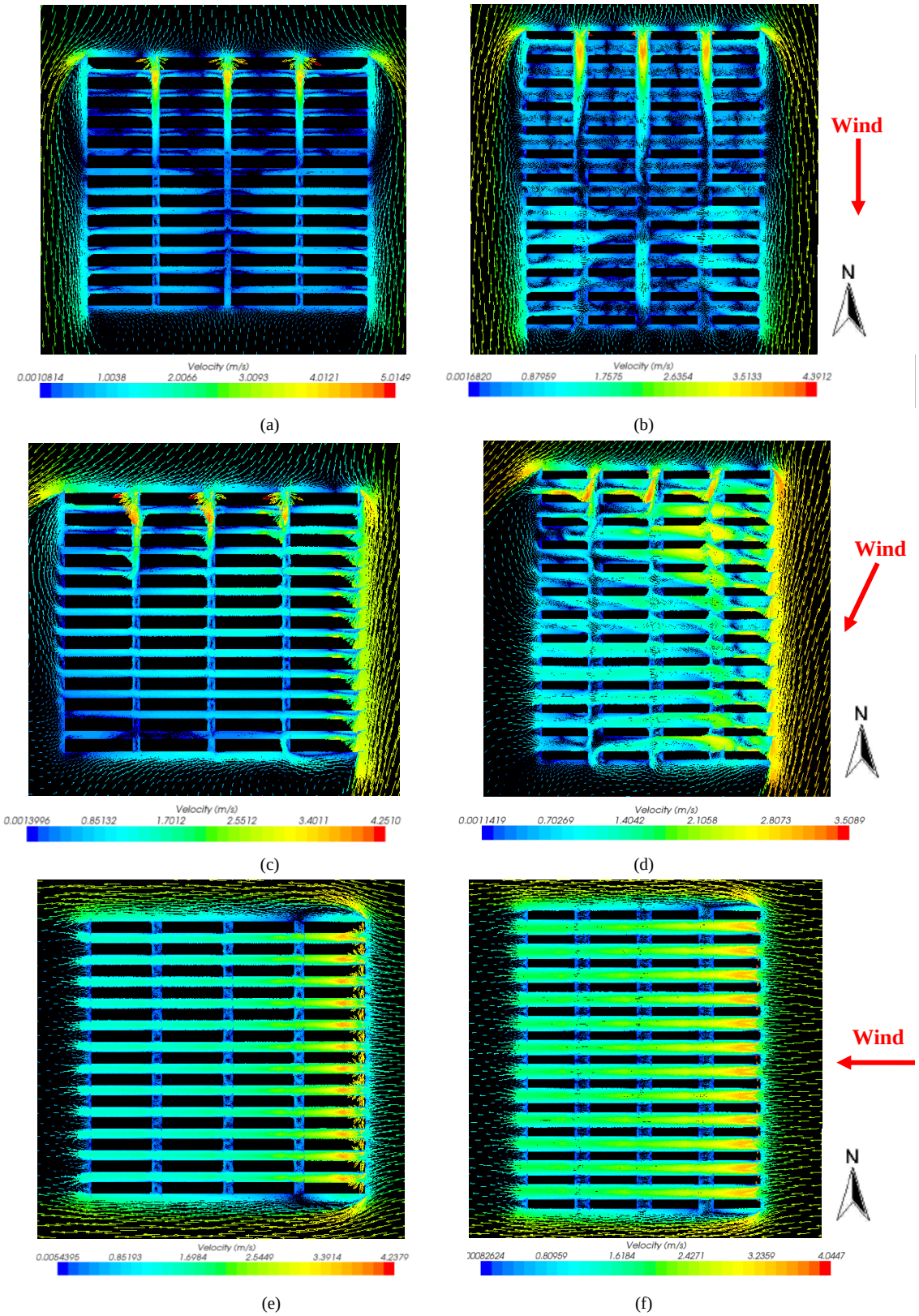

Fig. 17 Slab blocks, geometric width variation (W) configuration:

(a) Velocity vectors for GEO = 21.09 (50m height, 10m width) for wind from 0˚ north (pedestrian level), plan view
(b) Velocity vectors for GEO = 46.42 (50m height, 30m width) for wind from 0˚ north (pedestrian level), plan view
(c) Velocity vectors for GEO = 21.09 (50m height, 10m width) for wind from 22.5˚ north (pedestrian level), plan view
(d) Velocity vectors for GEO = 46.42 (50m height, 30m width) for wind from 22.5˚ north (pedestrian level), plan view
(e) Velocity vectors for GEO = 28.97 (50m height, 15m width) for wind from 90˚ north (pedestrian level), plan view
(f) Velocity vectors for GEO = 46.42 (50m height, 30m width) for wind from 90˚ north (pedestrian level), plan view

V_R readings for 67.5˚ and 90˚ north orientations are quite constant throughout the range of GEO increase. It is possible that the canyon width has reached the threshold value early and any further increase will not provide any increase in V_R from the increase in mass flow rate. For example, Figs. 17e and 17f shows the difference in flow patterns between GEO = 28.97 (50m height, 15m width) and GEO = 46.42 (50m height, 30m width), respectively for 90˚ north wind orientation (Figs. 17e and 17f). In Fig. 17e, the configuration of GEO = 28.97 has 15m wide canyons and the velocity vectors seem to be more concentrated within the canyon indicating that some channeling effects may come into play. But in Fig. 17f, the configuration of GEO = 46.42 has 30m wide canyons and the velocity vectors seem to be quite diffused at the pedestrian level indicating that even though mass flow rate may increase with wider canyons, it seems that some potential channeling effects have lost as GEO progressively increases. The increased mass flow rate coupled with a corresponding decrease in potential channeling effects caused V_R to remain platonic as GEO increases.

E. Slab Blocks, Mid-Level

The overall results for area-averaged V_R values within the estate for slab blocks under the geometrical height variation (H) and geometrical width variation (W) GEO configurations are shown in Fig. 18 for mid-level.

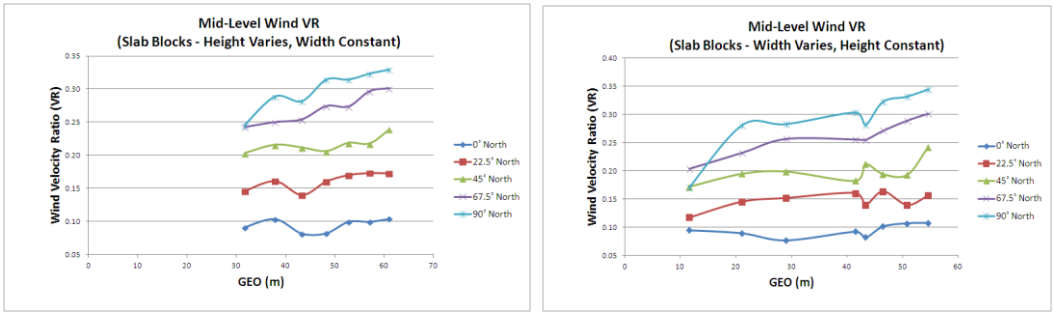

(a) (b)

Fig. 18 Mid-level area-averaged V_R against GEO for (a) geometric height variation (H) and (b) geometric width variation (W) configurations of slab blocks

1) Slab Blocks, Mid-Level – Geometrical Height Variation (H) Configuration:

V_R readings for all the wind orientations increase steadily as GEO increases (Fig. 18a). The reason for the increase is similar to the case for ***Slab Blocks, Pedestrian Level – Geometrical Height Variation (H) Configuration***.

The gradient of V_R increase gets progressively larger from 0˚ to 90˚ north wind orientation. Orientations which have larger number of canyons parallel or oblique to the wind orientation (lesser blockage) will have steeper gradient of V_R increase as GEO increases. For example in 67.5˚ wind orientation cases, Fig. 19a shows the velocity vectors of the wind flow for GEO = 31.68 (30m height, 20m width) and Fig. 19b shows the velocity vectors for GEO = 52.72 (70m height, 20m width) (Figs. 19a and 19b). People can see a significant increase in wind flow with increase in GEO from the former to the latter, due to the larger number of canyons facing the wind. For the same configuration of GEO = 31.68 (30m height, 20m width) (Fig. 19c) and GEO= 52.72 (70m height, 20m width) (Fig. 19d) for 0˚ north orientation, we can see that the magnitude of V_R increase from GEO = 31.68 to 52.72 is not as significant as 67.5˚ north wind orientation cases. The significant increase in wind flow with increase of GEO for 90˚ north wind orientation case is due to the largest number of canyons facing the wind and having the least massive wall areas (blockages).

For cases with more canyons parallel or oblique to the wind direction, the V_R readings are higher than those at the pedestrian levels (e.g. 67.5˚ and 90˚ north). The power-law wind profile that comes in parallel to the main canyons allows the highest degree of channeling with wind being the strongest at higher levels. For the other orientations, the V_R readings for mid-levels are close but slightly higher than those at the pedestrian levels. This is due to the higher degree of blockages from the massive wall facing the 0˚ north orientation and lesser number of canyons parallel or oblique to the wind direction. These hamper positive wind flow into a precinct. As expected, V_R magnitude increases progressively from 0˚ to 90˚. The high values of V_R at mid-levels are related to the most number of canyons parallel to the wind flow.

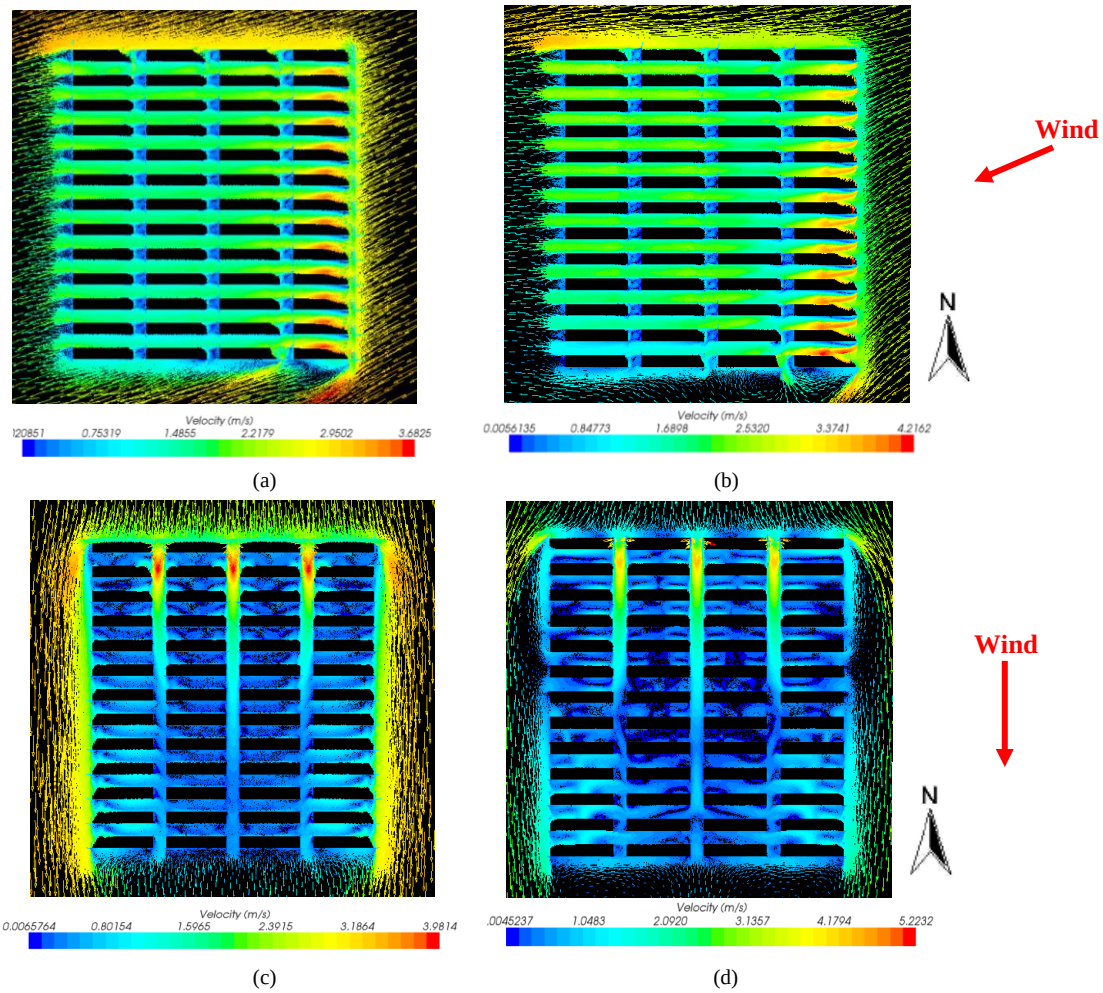

Fig. 19 Slab blocks, geometric height variation (H) configuration:

(a) Velocity vectors for GEO = 31.68 (30m height, 20m width) for wind from 67.5˚ north (mid-level), plan view
(b) Velocity vectors for GEO = 52.72 (70m height, 20m width) for wind from 67.5˚ north (mid-level), plan view
(c) Velocity vectors for GEO = 31.68 (30m height, 20m width) for wind from 0˚ north (mid-level), plan view
(d) Velocity vectors for GEO = 52.72 (70m height, 20m width) for wind from 0˚ north (mid-level), plan view

2) Slab Blocks, Mid-Level – Geometrical Width Variation (W) Configuration:

In the geometric width variation (W) configuration for slab blocks at mid-level, V_R readings for all wind orientations increase steadily as GEO increases (Fig. 18b). This increase is due to the increase in mass flow rate from the increase in canyon width. The rest of the V_R behavioral patterns and the reasons behind are similar to that of Slab Blocks, Mid-Level – Geometrical Height Variation (H) Configuration.

F. Slab Blocks – Combined Results of Geometrical Height (H) and Width (W) Variation

Fig. 20 shows the combined results of GEO variations for both geometric height (H) and width (W) variation at pedestrian and mid-levels for slab blocks. We can see that the overall V_R results show an increasing trend with increasing GEO variation.

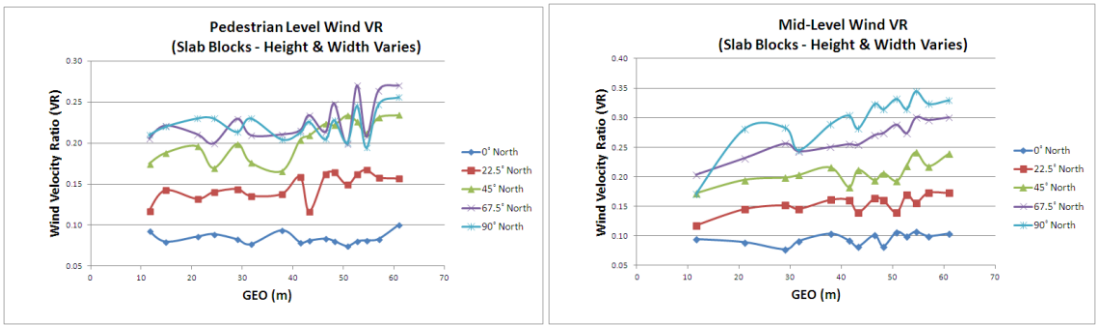

Fig. 20 Pedestrian and mid-levels area-averaged V_R against GEO for combined geometric height variation (H) and geometric width variation (W) configurations of slab blocks

IV. CASE STUDIES

The increase in GEO (quantified by the HD_{Max}) will almost always lead to an increase in V_R within the precinct at a certain level above ground. This behaviour will be demonstrated in the following case studies in this section. The main case study consists of a newly proposed upcoming HDB precinct development at the initial design stage, of which actual construction works have not started yet. This proposed new precinct will consist of mostly slab blocks, a few point blocks and multi-storey car parks to service car owners living within the precinct. A few possible variable proposals have also been drawn up for full consideration of their merits and most importantly, their ventilation potential for the entire estate. In this study here, a main base proposal will be put up and apart from this, other alternative scenarios will also be considered. These proposed alternative scenarios are:

1. Increasing the building height of all the HDB blocks, including the car parks.
2. Decreasing the spacing between all HDB blocks, including the car parks.

This proposed new precinct for the main base case consists of mostly slab blocks, four point blocks (highlighted in pink) in the middle of the precinct and two multi-storey car parks (Fig. 21). Fig. 21 shows the plan view of the proposed precinct and Fig. 22 shows the 3D perspective view (Figs. 21 and 22). The basic information of this base case design proposal is shown in Table 5. In the subsequent two alternative proposals, some of these quantities will be varied in order to compare the effects of each morphological change. Basically the cross-sectional footprint area of each individual HDB block and car park within the precinct will remain the same throughout all study cases.

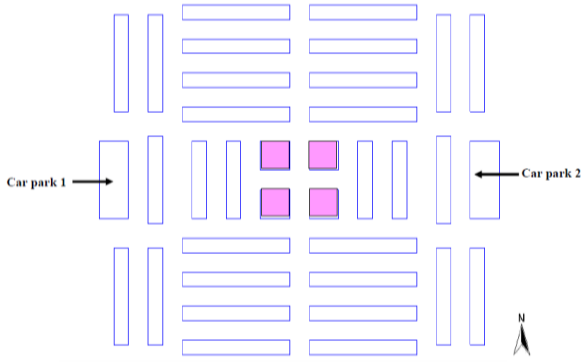

Fig. 21 Proposed HDB precinct base design layout plan; point blocks are highlighted in pink (base case)

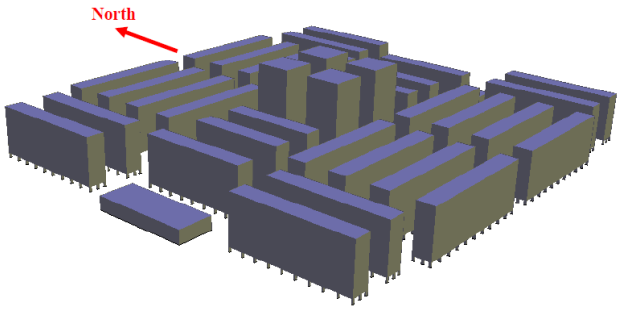

Fig. 22 Perspective view of proposed HDB precinct base design

TABLE 5 BASIC INFORMATION ABOUT THE PROPOSED BASE HDB PRECINCT DESIGN

Description	Value	Unit
No. of storeys of each HDB slab block	14.00	storey
No. of storeys of each HDB point block	25.00	storey
Height of each HDB block storey (standard)	2.80	metres
Spacing between the blocks	20.00	metres
Height of HDB void decks	3.60	metres
No of storeys of each car park	4.00	storey
Height of each carpark storey (standard)	2.80	metres

According to the current mandatory HDB design requirements, if there is a provision of void decks at ground level, the floor to floor height for the ground floor void deck shall be of minimum of 3.6m high [42]. Since we do not have the exact layout of the columns at this moment, an assumption is made that each oblong column is round 2.00m by 1.00m with spacing of around 10.00m according to the HDB requirements. For a typical storey height of an apartment block, the minimum floor to

floor height shall be of 2.8m high [42]. Pitched roofs which are mostly tiled, are not encouraged for HDB blocks which are above five storeys high. This is to avoid any unforeseen incidents such as falling objects and likewise for metal-pitched roofs, to avoid unforeseen incidents such as flying roof. Hence, all blocks in this proposed base design are to be constructed as flat-roofed.

A. Increase in Building Height

The first alternative scenario consists of an increase in building height of all the HDB blocks, including the car parks. The advantage of this proposal is the ability to accommodate a higher number of residents (subject to development and demographics control). This also inevitably leads to an increase in car parking space as well. The plan view of this proposal is similar to the base case scenario and Fig. 23 shows the 3D perspective view of this proposal (Fig. 23). The basic information of this alternative design with higher building heights is shown in Table 6. The quantities that were highlighted in yellow differ from those of the base case. The cross-sectional footprint area of every HDB block and car park within the precinct remains the same as the base case scenario.

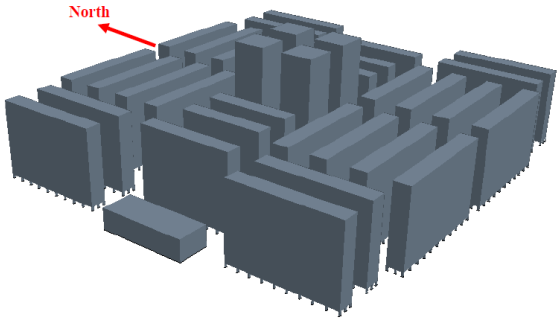

Fig. 23 Perspective view of proposed HDB precinct alternative design with higher building heights

TABLE 6 BASIC INFORMATION ABOUT THE PROPOSED ALTERNATIVE HDB PRECINCT DESIGN WITH HIGHER BUILDING HEIGHTS

Description	Value	Unit
No. of storeys of each HDB slab block	25.00	storey
No. of storeys of each HDB point block	40.00	storey
Height of each HDB block storey (standard)	2.80	metres
Spacing between the blocks	20.00	metres
Height of HDB void decks	3.60	metres
No of storeys of each car park	7.00	storey
Height of each carpark storey (standard)	2.80	metres

B. Decrease in Spacing between the Blocks

The second alternative scenario consists of a decrease in spacing between all the blocks, including the car parks. The objective of this proposal is to gauge how much the wind flow levels will be affected by a decrease in canyon width between the buildings. If the effect is not significant, planners might consider it as a space saving option whereby additional blocks within the precinct can be built. The plan view of this alternative proposal is different from the base case due to the narrower canyon spaces and is shown in Fig. 24 (Fig. 24). Fig. 25 shows the 3D perspective view of this proposal (Fig. 25).

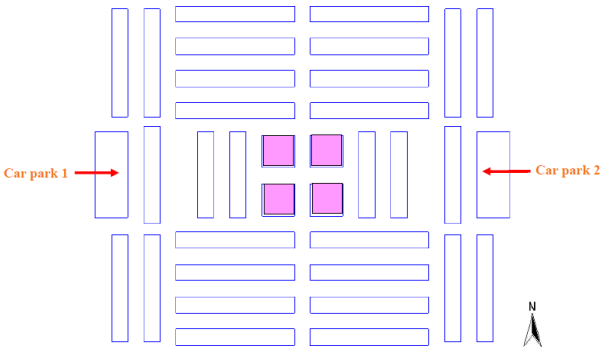

Fig. 24 Proposed HDB precinct design layout plan with narrower spacing (canyons) between the blocks; point blocks are highlighted in pink

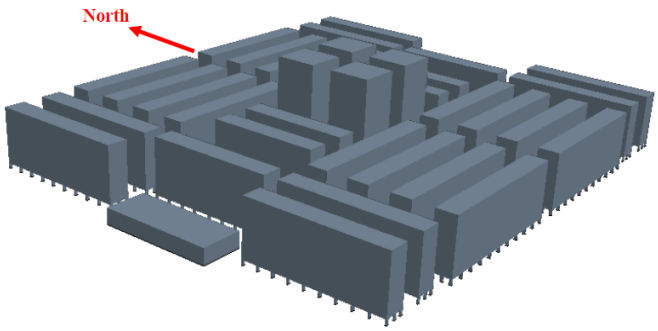

Fig. 25 Perspective view of proposed HDB precinct alternative design with narrower spacing (canyons) between the blocks

The basic information of this alternative design is shown in Table 7. The quantities that were highlighted in yellow differ from those of the base case. The cross-sectional footprint area of each and every HDB block within the precinct will remain the same as the base case scenario.

TABLE 7 BASIC INFORMATION ABOUT THE PROPOSED ALTERNATIVE HDB PRECINCT DESIGN WITH NARROWER SPACING (CANYONS) BETWEEN THE BLOCKS

Description	Value	Unit
No. of storeys of each HDB slab block	14.00	storey
No. of storeys of each HDB point block	25.00	storey
Height of each HDB block storey (standard)	2.80	metres
Spacing between the blocks	20.00	metres
Height of HDB void decks	6.40	metres
No of storeys of each car park	4.00	storey
Height of each carpark storey (standard)	2.80	metres

C. Mapping of GEO Quantities

The mapping of GEO quantities for base case scenario will be explained briefing in this section for appreciation of its use. The same techniques are applicable for mapping other scenarios as well. In order to determine the mid-level in situations where you encounter a mixture of point and slab blocks, some of the rules are as follows:

- If there is a high proportion of slab block within the precinct, we use 25m and likewise for point blocks, we use 56m. E.g. 80% and above for each block type.
- If there is an obvious mixture of point and slab blocks, the proportion of blocks types will be prorated to work out the height in between 25m and 56m.

The mid-level that is used in this base case study is 25m, following the parametric study for slab blocks. This is due to the base case having a much higher number of slab that point blocks, otherwise the mid-height will be pro-rated between 25m and 56m, based on the percentage of point or slab blocks within the precinct. Furthermore, the average height of all buildings within the precinct worked out to be around 44.47m which is smaller than the parametric study for point blocks at mid-level which is 56m.

The morphological index that is used to quantify Geometry (GEO) is the Maximum Hydraulic Diameter (HD_{Max}), which is defined as the summation of all the largest hydraulic diameter (HD) of individual outdoor grid space, that are each area-weighted over the whole given precinct area. The HD_{Max} can be worked out with this formula: HDMax = Σ [(Largest HD of Area *i*)*(% of Area *i* in Precinct)]. The details of the calculation method have been explained in the Section 2, Part A. Fig. 26 shows the canyon areas that are not covered by the buildings' footprint, highlighted in different colors to identify the individual outdoor grid space (Fig. 26). The numbers on the top of the blocks indicated the individual height of each building. The single hashed lines mean that the area is affected by one pair of upwind and downwind buildings. Double hashed lines means that the area is affected by two pairs of upwind and downwind buildings. The larger hydraulic diameter (HD) worked out from both transverse directions are used to work out the HD_{Max}. Those uncolored areas within the perimeter outline will be considered as 'empty' non-canyon spaces and be subjected to the highest HD whereby the longer side of the perimeter enclosure i.e. 392m and the average height of all buildings within the precinct are used to work out their HDs (Fig. 26).

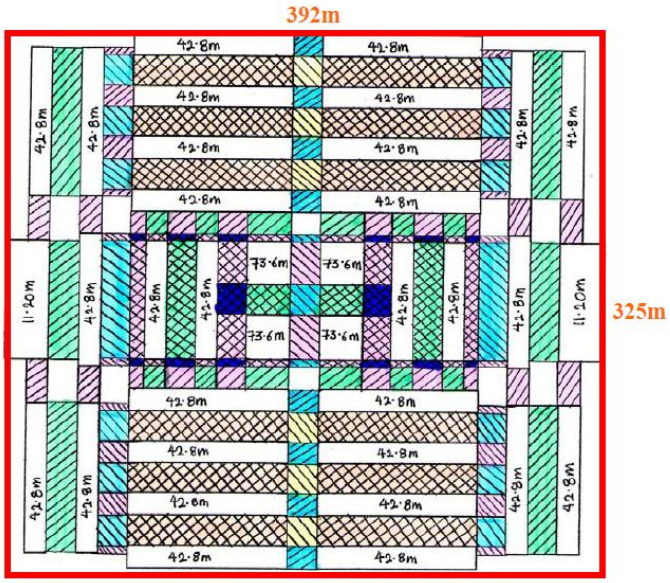

Fig. 26 Plan view of proposed HDB precinct base design indicating the perimeter outline of the enclosed precinct area and individual outdoor grid space

D. Results and Discussion

1) Increase in Building Height

The results of the readings for building height increase compared to the base case scenario are shown in Fig. 27. We noticed that the mid-level readings are higher than those of pedestrian level. When people compare the V_R readings for building height increase scenario with the base case, the former one show only a slight average improvement in V_R values of about 0.01 for pedestrian level; whereas for mid-level, the average improvement is higher at about 0.03. The increase in building heights (increase in GEO) in this case, leads to an increase in channeling effects where wind speeds are higher compared to the base scenario. The presence of the void decks at ground level might have narrowed down the differences between these two scenarios at ground level; whereas for mid-level, there are no porosity like sky gardens to achieve that. In other words, the void decks in the base scenario help to improve the ventilation potential first even before there are any channeling effects from the increase in building height.

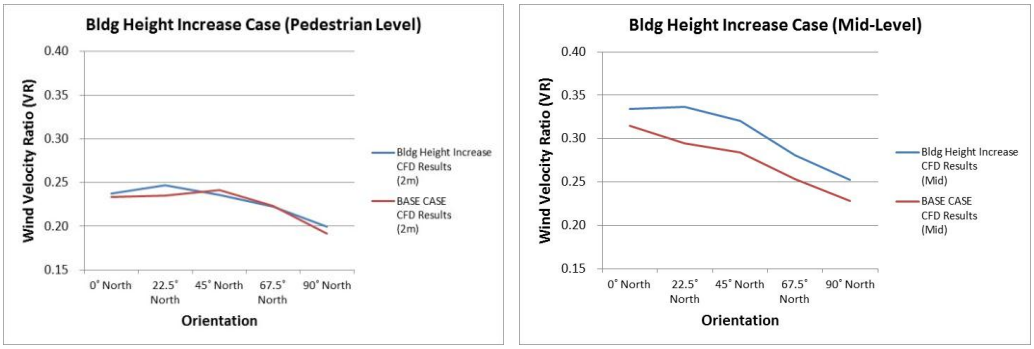

(a) (b)

Fig. 27 Comparison of V_R readings for increase in building height case scenario at (a) pedestrian level and (b) mid-level

Fig. 28 shows the velocity magnitude scalar diagrams at both pedestrian and mid-levels for 0 °north orientation wind in the increase in building height scenario (Fig. 28). When this is compared to the base case scenario as shown in Fig. 29 at these two levels, we can see that the former scenario seems to possess more channeling effects of the wind due to the taller buildings which also serves to increase the GEO index by virtue of an increase in hydraulic diameter of the canyon space between the adjacent buildings (Figs. 28 and 29).

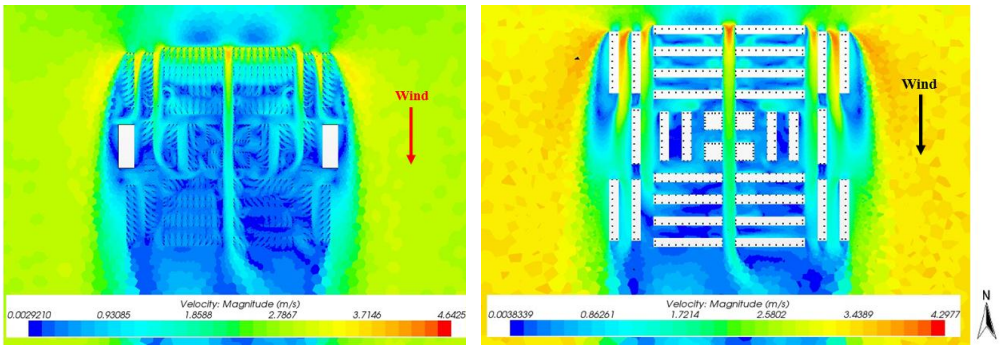

(a) (b)

Fig. 28 Velocity magnitude scalar diagrams for the increase in building height scenario at (a) pedestrian level and (b) mid-level for 0 °north wind orientation

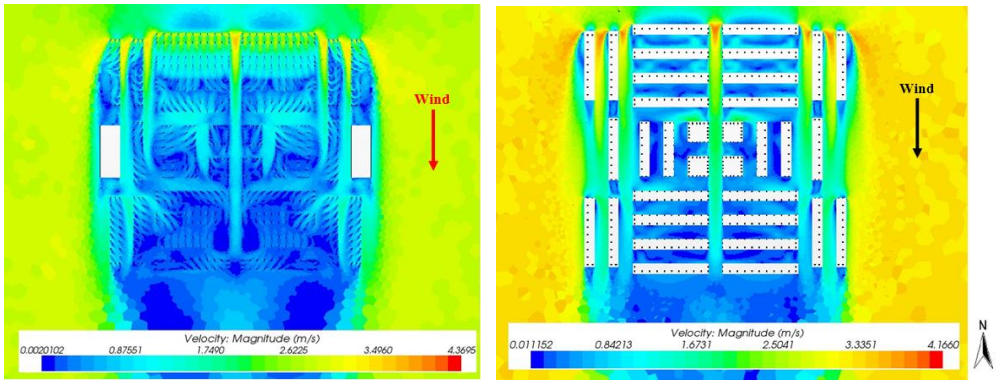

(a) (b)

Fig. 29 Velocity magnitude scalar diagrams for base case scenario at (a) pedestrian level and (b) mid-level for 0 °north wind orientation

2) Decrease in Spacing between the Blocks

The results of the readings for decrease in spacing between the blocks compared to the base case scenario are shown in Fig. 30 (Fig. 30). We noticed that the mid-level readings are higher than those of the pedestrian level. When we compare the V_R readings for decrease in blocks spacing scenario with the base case, the decrease in spacing (decrease in GEO) between the blocks scenario shows an average decrease in V_R values of less than 0.01 for both the pedestrian and mid-levels which is not really a significant decrease. At the pedestrian level, the presence of void decks which allow more wind to flow into the precinct tends to further narrow down any differences between the two different scenarios. The higher turbulence at mid-level tends to 'mask' away any slight differences between the readings as well. It seems that the decrease in 5m spacing does not really lower down the V_R reading which means that the additional areas at a given precinct could be used for communal facilities or to build additional HDB blocks, but subjected to development controls.

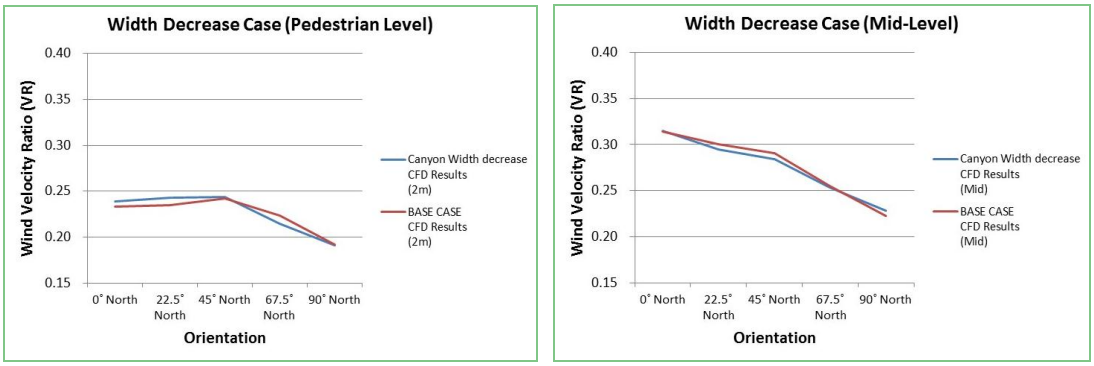

(a) (b)

Fig. 30 Comparison of V_R readings for decrease in spacing between blocks case scenario at (a) pedestrian level and (b) mid-level

Fig. 31 shows the velocity magnitude scalar diagrams at both pedestrian and mid-levels for 0 °north orientation wind in the decrease in spacing between blocks scenario (Fig. 31). When this is compared to the base case scenarios (Fig. 29) at these two levels, there are not many differences in the distribution of velocity magnitude values. In general, a 5m decrease in all canyon widths does not significantly decrease the V_R readings.

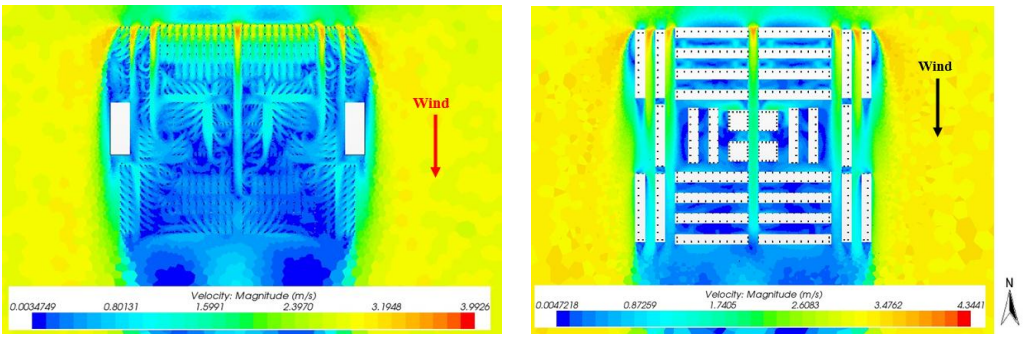

(a) (b)

Fig. 31 Velocity magnitude scalar diagrams for the decrease in spacing between blocks scenario at (a) pedestrian level and (b) mid-level for 0 °north wind orientation

V. CONCLUSIONS

The detailed parametric and case studies that was carried out to investigate the association of GEO (calculated by HD_{Max}) with the area-averaged V_R index within a high-rise HDB residential estate, was carried out through the use of numerical simulations. The impact of different morphological scenarios of GEO variations were studied for both geometric height (H) and width (W) variations for both point and slab block types. The results generally show that the increase in GEO gives an overall increase in V_R results.

The geometric height variation (H) studies for both point and slab blocks showed that the increase in buildings' height does not necessarily lead to poor ventilation at both pedestrian and mid-levels. This is due to the presence of channeling effects but provided that the canyon width is not too narrow for the range of geometric height increase. Orientations with more canyons that are more parallel towards the wind direction have higher degree of channeling effects; hence they have generally higher V_R magnitudes and/or gradient of increase. The other reason is due to the progressive reduction in massive wall area blockages. Next, the geometric width variation (W) studies for both point and slab blocks showed that the increase in width of canyons (GEO increase) leads to an increase in V_R. This is basically due to the increase in mass flow rate from the increase in canyon width, which is different from the channeling effects as mentioned for geometric height variation (H). The continual increase in GEO will reach a point when V_R values for all wind orientations started to plateau from further GEO increase (increase in canyon width). It has reached a threshold value whereby further increase does not provide any further channeling or increased mass flow rate due to their predominantly stabilized near wake-interference or isolated-roughness wind flow structures. In addition, when there are more canyons parallel towards the wind direction, V_R readings at mid-levels are higher than those at the pedestrian level. This is due to the power-law wind profile which comes in parallel to the main canyons and this allows the highest degree of channeling with wind being stronger at higher levels.

From this parametric study, we can see that under different types of GEO variations, we can observe different types of ventilation level at both the pedestrian and mid-levels. The variations also comes from other factors like wind orientation and building shapes as well. But nevertheless, one thing that is consistent about the behavior is that the increase in GEO (quantified by the HD_{Max}) will almost always lead to the increase in V_R within the precinct at a certain level above ground. In the use of HD_{Max} to quantify GEO, problems like scaling in aspect ratios, and inconsistent treads in the progressive variation of these aspect ratios can be overcome. The results from this study have important implications for building and urban planning development of residential estates in future. For example, under certain circumstances when there is limited area of land for development with a certain height limit, the planner can consider how high the buildings can go and how far apart the buildings are advisable, so as to achieve good ventilation potential for the overall estate. Due consideration of other morphological variables will also be needed as well.

The consistent trends in this study supports the possibility of using GEO to develop an overall ventilation potential model which also considers other morphological variables mentioned as independent variables. The V_R will be used as the dependent variable, an indication of estate-level outdoor ventilation potential. This model will provide some useful prediction of how GEO, together with other morphological values, will affect the estate's ventilation. This will be useful for pinpointing problematic designs during early stage and also making comparisons between different proposals. It is hoped that the data in this detailed simulation study of GEO can be used for subsequent development of this overall ventilation model which will be useful for urban planning of high-rise precincts by building professionals.

NOMENCLATURE

α: Power-law exponent

BCA: Building and Construction Authority

BLWT: Boundary layer wind tunnel

CFD: Computational Fluid Dynamics
CUHK: Chinese University of Hong Kong
GBCR: Gross Building Coverage Ratio
GEO: Geometry
H: Height of building
HD: Hydraulic Diameter
HD_{Max}: Maximum Hydraulic Diameter
HDB: Housing and Development Board
IRF: Isolated roughness flow
L: Longitudinal length of building
NEA: National Environment Agency
RANS: Reynolds-averaged Navier-Stokes
RLZ: Realizable k-ε turbulence model
Re: Reynolds number
SF: Skimming flow
UBL: Urban boundary layer
UCL: Urban canopy layer
V_R: Wind Velocity Ratio
W: Width between buildings
WIF: Wake interference flow
Z_0: Roughness length

REFERENCES

[1] M. Santamouris, *Energy and Climate in the Urban Built Environment*, UK: James and James (Science Publishers) Ltd, 2001.

[2] L. J. Hunter, G. T. Johnson, and I. D. Watson, "An investigation of three-dimensional characteristics of flow regimes within the urban canyon," *Atmospheric Environment*, vol. 26B, iss. 4, pp. 425-432, 1992.

[3] L. Adolphe, "A simplified model of urban morphology: application to an analysis of the environmental performance of cities," *Environment and Planning (B): Planning and Design*, vol. 28, iss. 2, pp. 183-200, 2001.

[4] J.-J. Kim and J.-J. Baik, "A numerical study of the effects of ambient wind direction on flow and dispersion in urban street canyons using the RNG k-ε turbulence model," *Atmospheric Environment*, vol. 38, iss. 19, pp. 3039-3048, 2004.

[5] E. Ng, "Policies and technical guidelines for urban planning of high-density cities – air ventilation assessment (AVA) of Hong Kong," *Building and Environment*, vol. 44, pp. 1478-1488, 2009.

[6] J. A. Roberson and C. T. Crowe, *Engineering Fluid Mechanics*, USA: Wiley, 1988.

[7] G. Z. Brown and M. Dekay Sun, *Wind and Light: Architectural Design Strategies*, 2nd ed., New York: Wiley, 2001.

[8] B. Givoni, *Climate Considerations in Building and Urban Design*, USA: Wiley, 1998.

[9] G. S. Golany, "Urban design morphology and thermal performance," *Atmospheric Environment*, vol. 30, iss. 3, pp. 455-465, 1996.

[10] T. Kubota, M. Miura, Y. Tominaga, and A. Mochida, "Wind tunnel tests on the relationship between building density and pedestrian-level wind velocity: Development of guidelines for realizing acceptable wind environment in residential neighborhoods," *Building and Environment*, vol. 43, iss. 10, pp. 1699-1708, 2008.

[11] T. R. Oke, "Street design and urban canopy layer climate," *Energy and Buildings*, vol. 11, iss. 1-3, pp. 103-113, 1988.

[12] A. Zhang, C-L. Gao, and L. Zhang, "Numerical simulation of the wind field around different building arrangements," *Journal of Wind Engineering and Industrial Aerodynamics*, vol. 93, pp. 891-904, 2005.

[13] L. J. Hunter, I. D. Watson, and G. T. Johnson, "Modeling air flow regimes in urban canyons," *Energy and Buildings*, vol. 15-16, iss. 3-4, pp. 315-324, 1990/1991.

[14] M. Hussain and B. E. Lee, "An Investigation of Wind Forces on Three-dimensional Roughness Elements in a Simulated Atmospheric Boundary Layer Flow – Part II. Flow Over Large Arrays of Identical Roughness Elements and the Effect of Frontal and Side Aspect Ratio Variations," *Report No BS 56, Department of Building Sciences*, University of Sheffield, 1980.

[15] J. F. Sini, S. Anquetin, and P. G. Mestayer, "Pollutant dispersion and thermal effects in urban street canyons," *Atmospheric Environment*, vol. 30, iss. 15, pp. 2659-2677, 1996.

[16] A. T. Chan, E. S. P. So, and S. C. Samad, "Strategic guidelines for street canyon geometry to achieve sustainable street air quality," *Atmospheric Environment*, vol. 35, iss. 32, pp. 5681-5691, 2001.

[17] X. Xie, Z. Huang, and J. S. Wang, "Impact of building configuration on air quality in street canyon," *Atmospheric Environment*, vol. 36, pp. 3601-3613, 2005c.

[18] R. W. MacDonald, R. F. Griffiths, and D. J. Hall, "An improved method for the estimation of surface roughness of obstacle arrays," *Atmospheric Environment*, vol. 32, iss. 11, pp. 1857-1864, 1998.

[19] M. R. Raupach, "Drag and drag partition on rough surfaces," *Boundary-layer Meteorology*, vol. 60, iss. 4, pp. 375-395, 1992.

[20] S. E. Nicholson, "Air pollution model for street-level air," *Atmospheric Environment*, vol. 9, iss. 1, pp. 19-31, 1975.

[21] S. Vardoulakis, B. E. A. Fisher, K. Pericleous, and N. Gonzalez-Flesca, "Modeling air quality in street canyons: a review," *Atmospheric Environment*, vol. 37, iss. 2, pp. 155-182, 2003.

[22] R. J. Yamartino and G. Wiegand, "Development and evaluation of simple models for the flow, turbulence and pollution concentration fields within an urban street canyon," *Atmospheric Environment*, vol. 20, pp. 2137-2156, 1986.

[23] W. G. Hoydysh and W. F. Dabberdt, "Kinematics and dispersion characteristics of flows in asymmetric street canyons," *Atmospheric Environment*, vol. 22, iss. 12, pp. 2677-2689, 1988.

[24] M. Santamouris, N. Papanikolaou, I. Koronakis, I. Livada, and D. N. Asimakopoulos, "Thermal and air flow characteristics in a deep pedestrian canyon and hot weather conditions," *Atmospheric Environment*, vol. 33, iss. 27, pp. 4503-4521, 1999.

[25] P. Kastner-Klein and E. J. Plate, "Wind-tunnel study of concentration fields in street canyons," *Atmospheric Environment*, vol. 33, pp. 3973-3979, 1999.

[26] W. Theurer, "Typical building arrangements for urban air pollution modeling," *Atmospheric Environment*, vol. 33, iss. 24, pp. 4057-4066, 1999.

[27] X. -X. Li, C. -H. Liu, D. Y. C. Leung, and K. M. Lam, "Recent progress in CFD modeling of wind field and pollutant transport in street canyons," *Atmospheric Environment*, vol. 40, iss. 29, pp. 5640-5658, 2006.

[28] R. X. Lee and N. H. Wong, "A parametric study of Gross Building Coverage Ratio (GBCR) variation on outdoor ventilation in Singapore's high-rise residential estates," *Journal of Civil Engineering and Science*, vol. 3, iss. 2, pp. 93-117, 2014.

[29] S. J. Burian, S. P. Velugubantla, and M. J. Brown, "Morphological Analyses Using 3D Building Databases: Phoenix, Arizona," Report No. LA-UR-02-6726, Energy and Environmental Analysis Group, Los Alamos National Laboratory, 2002.

[30] R. X. Lee, S. K. Jusuf, and N. H. Wong, "The study of height variation on outdoor ventilation for Singapore's high-rise residential housing estates," *International Journal of Low-Carbon Technologies*, vol. 0, pp. 1-19, 2013.

[31] T. -H. Shih, W. W. Liou, A. Shabbir, Z. Yang, and J. Zhu, "A new k-ε eddy viscosity model for high Reynolds number turbulent flows," *Computer Fluids*, vol. 24, iss. 3, pp. 227-238, 1995.

[32] T. L. Chan, G. Dong, C. W. Leung, C. S. Cheung, and W. T. Hung, "Validation of a two-dimensional pollutant dispersion model in an isolated street canyon," *Atmospheric Environment*, vol. 36, iss. 5, pp. 861-872, 2002.

[33] H. W. Han, "A study of entrainment in 2-phase upward concurrent annular flow in a vertical tube," PhD Thesis, University of Saskatchewan, 2005.

[34] C. Teodosiu and G. Rusaouen, "Modelisation des corps de chauffe a l'aide des codes de champ," *Proceedings of the Fourth Fluent Users Meetings – France*, Paris, France, 2000.

[35] J. C. DeBlois, M. M. Bilec, and L. A. Schaefer, "Design and zonal building energy modeling of a roof integrated solar chimney," *Renewable Energy*, vol. 52, pp. 241-250, 2013.

[36] Building and Construction Authority (BCA), Code for Environmental Sustainability of Buildings, 3rd ed., Singapore: BCA, 2012.

[37] COST (Best Practice Guidelines for the CFD Simulation of Flows in the Urban Environment) - COST Action 732 (Quality Assurance and improvement of microscale meteorological models), University of Hamburg, Meteorological Institute, Centre for Marine and Atmospheric Sciences, Hamburg, Germany, 2007.

[38] B. C. Cochran, "The Influence of Atmospheric Turbulence on the Kinetic Energy Available During Small Wind Turbine Power Performance Testing," *IEA Expert Meeting on: Power Performance of Small Wind Turbines Not Connected to the Grid*, CEDER-CIEMAT, Soria, Spain, 2002.

[39] J. Wieringa, "Updating the Davenport roughness classification," *Journal of Wind Engineering and Industrial Aerodynamics*, vol. 41, iss. 1-3, pp. 357-368, 1992.

[40] F. T. De Paul and C. M. Shieh, "Measurements of Wind Velocities in a Street Canyon," *Atmospheric Environment*, vol. 20, iss. 3, pp. 455-459, 1986.

[41] CUHK, Urban Climatic Map and Standards for Wind Environment – Feasibility Study Working Paper 1A: Draft Urban Climatic Analysis Map, 2008.

[42] Housing and Development Board (HDB), Proposed Public Housing Development Under the Design, Build and Sell Scheme – Particulars and Conditions of Tender, Singapore: HDB, 2004.